Modeling Steady-State Suspension Kinematics and Vehicle Dynamics of Road Racing Cars - Part I: Theory and Methodology

Author(s): Thomas C. Crahan

Source: *SAE Transactions*, 1996, Vol. 105, Section 2: JOURNAL OF COMMERCIAL VEHICLES (1996), pp. 1-34

Published by: SAE International

Stable URL: https://www.jstor.org/stable/44718244

942505

Modeling Steady-State Suspension Kinematics and Vehicle Dynamics of Road Racing Cars - Part I: Theory and Methodology

Thomas C. Crahan

ABSTRACT

This paper presents basic suspension kinematics & vehicle dynamics concepts along with the equations necessary to model the steady-state handling behavior of road racing cars on a personal computer. Definitions for roll center, the roll resistance contribution of springs & anti roll bars, and instantaneous motion ratios are refined. These refined definitions correct several assumptions present in the classic design methods which lead to erroneous modeling results. These design methods and modeling equations are valid for the unequal length non-parallel type passive suspensions commonly found in competition vehicles.

This paper is part one in a two part series. The second paper (SAE Paper #942506) includes the design specifications and modeling results for a CART Indy car, IMSA GTS car and two Formula Fords. The computer model used to study the handling behavior of these cars was created with the methods and equations described in part one.

I) INTRODUCTION

This paper provides the reader with a basic understanding of road racing car suspension design using computer modeling as a learning tool. The information gap which currently exists between the classic texts on this subject, and modern computational methods is addressed by providing the reader with a step-by-step design process. This includes basic suspension kinematics and vehicle dynamics theory and the equations necessary to model the steady-state handling behavior of a road race car on a personal computer.

This paper does not attempt to cover the entire subject of racing car handling performance. It is rather a presentation of the essential concepts, related mathematics, and modeling examples which provide the engineer with a baseline data set for three popular racing classes that use passive suspensions.

II) SUSPENSION BASICS

2.10 TIRE OPERATIONAL PARAMETERS - While tire theory is outside the scope of this paper, a brief explanation of tire operational parameters will be discussed due to their significance on handling.

A principal goal of any competition suspension is to maintain a proper tire attitude with respect to the ground, while dealing with the complex external influences from chassis motion and load transfer. Another important goal which can dominate suspension design (depending on class rules) is to optimize aerodynamic performance by maintaining a constant vehicle attitude. Aerodyanamic requirements were a driving force for the development of active suspensions, however these suspensions will not be covered here.

Tires take on many non-cylindrical shapes as they are deformed by external and internal loads. Suspension systems are designed to compensate for these loads and deformations to maximize a tire's adhesion.

Tires are limited in the amount of total adhesion they can develop in any one direction. The balance between the longitudinal and lateral forces which they generate is commonly depicted with a *Coefficient of Friction Circle* (Figure 2.1). As Figure 2.1 shows, any adhesion used in one direction of operation, is reduced in the other direction. Tires are generally capable of generating more force longitudinally than laterally, therefore the *Coefficient of Friction Circle* is not truly circular, but elliptical. The radius of the ellipse defines the maximum adhesion force the tire is capable of generating in any one direction. To maximize the possible adhesion in both directions, it is critical that the tire operates in its optimum state. The primary factors which define this optimum state follow.

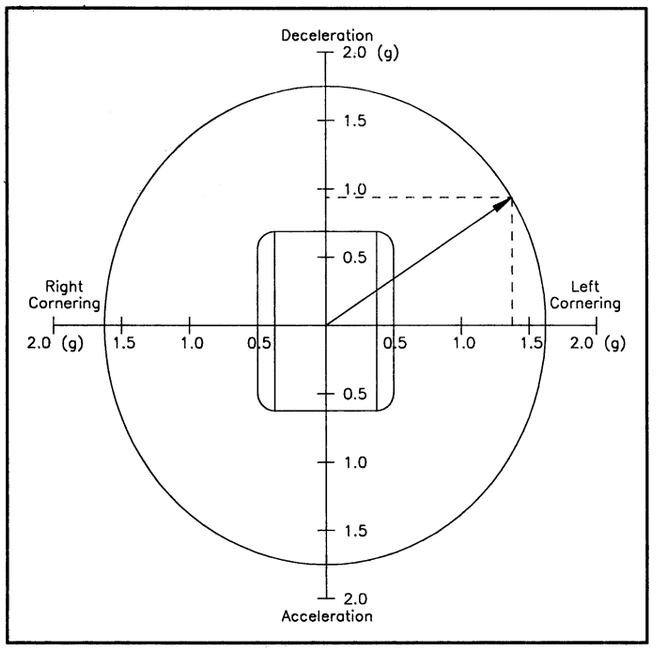

FIGURE 2-1

COEFFICIENT OF FRICTION CIRCLE

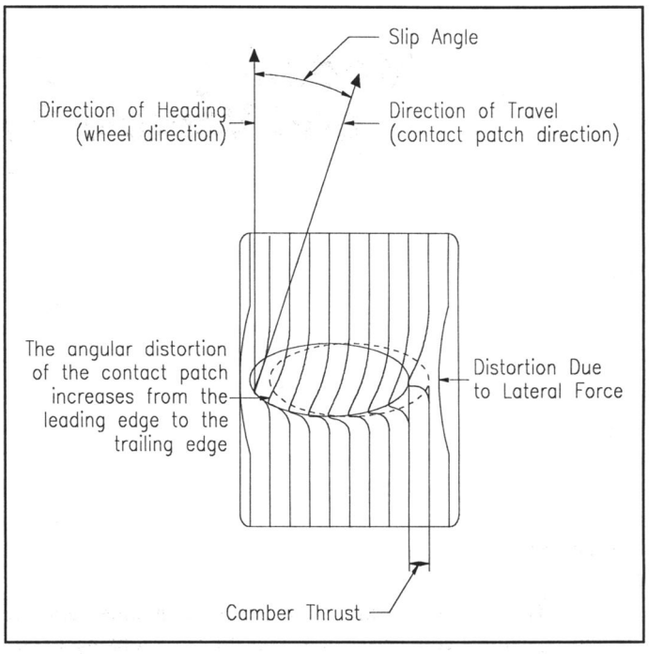

FIGURE 2-2

TIRE SLIP ANGLE

2.11 Slip Angle - Slip angle of a tire is the angular displacement between the direction in which the tire is pointing and the direction in which the tire contact patch is traveling (seen in Figure 2-2). As the tread rolls over the road surface while undergoing steering input, the tread particles become increasingly angularly distorted. These particles deflect from an undisturbed direction of heading to a disturbed direction of travel. As the tread particles become laterally distorted, the tread and sidewalls generate resistive forces to maintain equilibrium between the tire and the road. This distortion increases until the lateral force acting on that particle exceeds the available friction and causes the particle to slip. The point of maximum lateral force potential occurs just before the initiation of slip. This point is located slightly behind the center of contact patch. Once the particles begin to slip, they quickly return back to their undisturbed direction of travel at the trailing edge of the contact patch.

The slip angle at which a tire generates its maximum coefficient of friction depends on its construction. Racing tires are designed to generate large friction coefficients at small slip angles so that the driver can generate high lateral accelerations early in the corner without waiting for the tire to "build up" lateral forces further into the corner. After the tire has reached its optimum slip angle, the friction coefficient levels off to provide the driver with a safety margin, and then decreases almost as quickly as it was generated.

2.12 Slip Ratio - Slip ratio (or % slip) is the ratio of the tangential velocity of the tire contact patch in rotation, and the forward velocity of the vehicle as measured in percent. This difference in velocity produces a longitudinal distortion in the contact patch. This distortion generates longitudinal forces during acceleration and braking by the same mechanisms which produce lateral forces in cornering.

2.13 Camber Thrust - Camber thrust is the lateral force created by a tire as it rolls over a road surface while vertically inclined. When the top of a tire is vertically inclined toward the centerline of the vehicle (negative camber), the inner sidewall compresses more than the outer sidewall. This leads to an uneven load distribution across the contact patch which generates a lateral force as the tire rolls. This condition slightly increases cornering capacity, while positive camber slightly decreases cornering capacity.

The cornering force generated by slip angle is significantly larger than the force generated by camber thrust. Therefore, any additional lateral force gained by increasing camber angle beyond manufacturer recommendations is outweighed by the dramatic loss of slip angle induced lateral force caused by the subsequent loss of contact patch and the uneven load distribution. This is one reason why most road racing tires should be operated at less than 1.5 degrees of dynamic camber.

2.14 Tire Temperature - As a tire distorts under external forces, its temperature increases. Tires produce maximum adhesion only within narrow temperature ranges. The ideal tire temperature depends on many factors. Consult with the tire manufacturer for recommendations before starting the suspension design process.

Tread temperature changes dramatically with vertical and lateral loads. They can peak in the range of 350 to 370 deg. F. and change at a rate of 50 degrees per second [*]. Considering the rapid rate at which tread temperature can change, a primary suspension goal should be to control the rate of lateral load transfer. Since peak tire temperatures can vary by 100 to 150 deg. F. from the outside to inside tires, separate readings should be made after both left and right hand corners[**]. Peak tire temperatures of 370 deg. F are typically represented by temperatures of 250 to 300 deg. F. when measured immediately after stopping in the pits[***].

Suspension geometry affects tread temperature distribution. High negative camber angles not only decrease the lateral force possible from slip angle, but also adversely bias the tread temperature toward the inner shoulder. To maximize the tire's adhesion, temperature variances across the tread should be minimized through alignment and tire pressure adjustments.

2.20 SUSPENSION GEOMETRY PARAMETERS -

2.21 Camber Angle - Camber angle is the lateral inclination of the tire in the transverse vertical plane as measured from the ground (seen in Figure 2-3). Negative camber inclines the top of the tire toward the centerline of the vehicle, and positive camber inclines the top of the tire away from the centerline. It is necessary to have a small amount (up to 1.5 degrees) of negative camber in the suspension to induce camber thrust. Changes in camber should be minimized during roll to reduce the loss of camber thrust and the change in tire tread load distribution during cornering.

2.22 Steering Axis Inclination (SAI) - SAI (also known as kingpin inclination) is the lateral inclination of the steering axis in the transverse vertical plane as measured from the ground (seen in Figure 2-3). Inclining the steering axis so that its intersection with the ground is close to the tread's center of pressure reduces the torque about the steering axis during forward motion. Proper SAI also reduces steering effort at rest and provides the driver with an appropriate amount of steering "weight" or resistance at speed. Large SAI angles in combination with positive caster however can reduce the contact patch surface area during turn-in by generating dynamic camber too quickly.

[*]&[**] Van Valkenburgh, Paul. Race Car Engineering & Mechanics. (Seal Beach, Ca: Paul Van Valkenburgh, 1986), p. 9.

[***] Van Valkenburgh, Paul. Race Car Engineering & Mechanics. (Seal Beach, Ca: Paul Van Valkenburgh, 1986), p. 8.

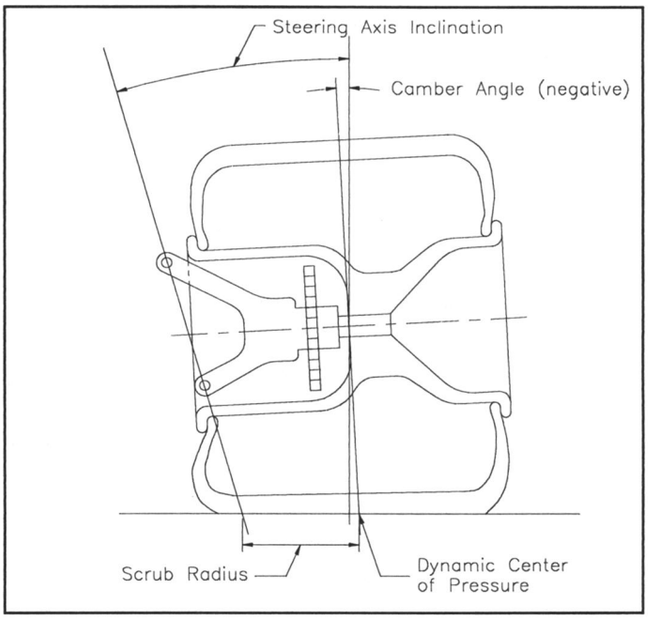

FIGURE 2-3

CAMBER ANGLE / STEERING AXIS INCLINATION / SCRUB RADIUS

2.23 Scrub Radius - Scrub radius is the distance (as measured on the ground plane) between the tread's center of pressure, and the intersection of the steering axis with the ground (seen in Figure 3-3). Scrub radius is positive when the center of pressure is outboard of the SAI's intersection with the ground. Scrub radius acts as a moment arm which induces a torque about the steering axis during forward motion. This torque promotes toe out conditions under braking and causes steering kickback. Because the dynamic center of pressure moves laterally and longitudinally when acted on by external forces and during camber change, scrub radius is typically measured at a static (zero degree camber) condition.

2.24 Caster - Caster angle is the longitudinal inclination of the steering axis from vertical as measured from the ground (seen in Figure 2-4). Positive Caster places the point at which the steering axis intersects the ground ahead of the treads' center of pressure. The moment arm between these two points produces a correcting torque which forces the tire towards a straight ahead position during forward motion. Caster ranges from approximately 2 degrees in racing vehicles up to 7 degrees in sedans.

Positive caster induces a self correcting force which provides straight line stability, but increases steering effort. Caster also increases camber angle during turn-in, especially when combined with large steering axis inclinations. This combination can quickly change camber angles, camber thrust and tread area. This combination can be used for generating the required level of camber at turn in, but should be used with restraint due to the possibility of non-linear understeer.

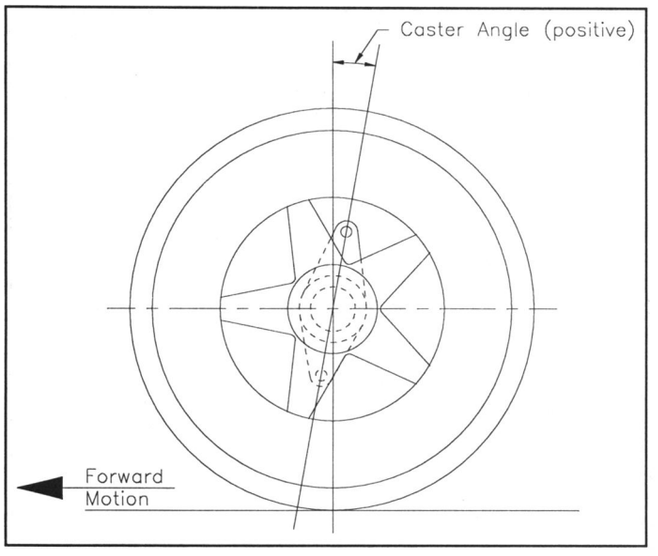

FIGURE 2-4

CASTER ANGLE

2.25 Toe - Toe is the angle in the plan view which the tire makes with the longitudinal axis. Toe is positive or "in" when the leading edges of the tires are closer than the trailing edges. Toe-in produces a constant lateral force inward toward the vehicle centerline during forward motion. This force enhances straight line stability. Static toe should be set such that the tires do not become toe "out" during maximum bump and roll. This will insure that the outboard laden tires do not steer the vehicle to the outside of the turn when cornering. This toe-out condition promotes understeer if it exists in the front, and oversteer if it exists in the rear. This bump steer effect should be avoided through proper suspension and steering kinematics.

III SUSPENSION KINEMATICS

Suspension kinematics is the study of suspension motions with respect to the vehicle and ground, and their effects on the dynamic behavior of the vehicle.

In general, purpose built road racing cars use unequal/non-parallel independent suspensions. The advantage of this design is that it reduces positive camber of the laden wheel during roll, and it gives the engineer the ability to design the appropriate roll center/camber control compromise. The characteristics of this suspension type will be covered, due to its current dominance in road racing.

3.10 SUSPENSION KINEMATIC PARAMETERS - In addition to the previously discussed geometrical parameters that are determined by design, suspension kinematics determines four other significant factors: instantaneous center, roll center, roll moment arm, & jacking forces.

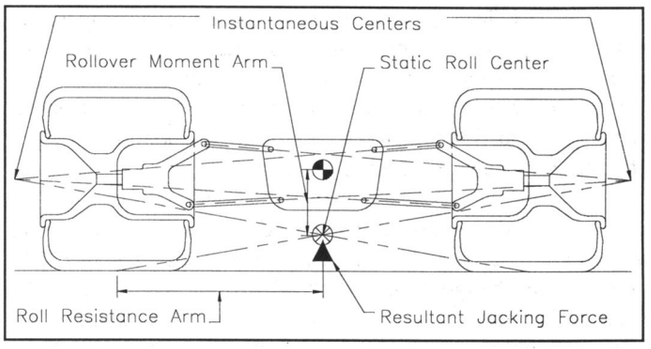

FIGURE 3-1

ROLL CENTER / ROLLOVER MOMENT ARM / JACKING FORCES

3.11 Instantaneous Center - The instantaneous center is the point in 2D space through which a body rotates at a given instant. In kinematic suspension analysis this instantaneous location is the point through which an individual wheel rotates. The instantaneous center of a suspension is also referred to as the "swing center" or "virtual half-shaft".

The instantaneous center of a four bar link independent suspension is located at the intersection of the upper and lower link extensions (as seen in Figure 3-1). Because these links are constantly rotating about their inner pick-up points, this intersection point (center of wheel rotation) is only valid at that instant. The instantaneous center is not only the point about which the respective wheel rotates, but is also the point through which the respective tire force acts on the sprung mass.

When analyzing suspension kinematics, both left and right suspensions must be analyzed together. Early models generally assumed symmetric behavior between the left and right halves of a suspension. This is an acceptable assumption for non-independent suspensions, but leads to large errors if used for the analysis of independent suspensions. When both sides are analyzed together, the resulting roll center of the complete suspension pair can be studied.

3.12 Roll Center - The suspension roll center is possibly the most dominant kinematic factor in the analysis and design of a suspension (seen in Figure 3-1).

Roll center is defined in SAE J670e as:

* "The point in the transverse vertical plane through any pair of *wheel centers* at which lateral forces may be applied to the sprung mass without producing *suspension roll*".

[*] SAE Vehicle Dynamics Committee. Vehicle Dynamics Terminology, SAE J670e. (Warrendale, PA: Society of Automotive Engineers, 1978)

The idealized definition given by SAE is misleading because it implicitly assumes that the horizontal position of the roll center is on the vehicle center-line. This is only correct for non-independent suspensions where both left and right suspension motions are symmetric. This is not a correct assumption for independent suspensions, especially as roll angle increases and left/right motions become less symmetric. This oversimplification leads to the following two problems:

A) Only the vertical position (or height) of the roll center is quantified when the roll center is defined in terms of a horizontal force applied to the sprung mass.

B) The additional rollover moment component (generated as the jacking forces act on the moment arm formed between the laterally displaced roll center and the vehicle center-line) is completely ignored when this lateral displacement is not accounted for.

Other authors define roll center as the point in space in the transverse plane of the axle through which the sprung mass rolls. This definition is incorrect because it necessitates that roll angle be calculated at the instantaneous position of the roll center. This would require that the vehicle rise tremendously for the measured roll angle to equal the roll angle calculated using this definition. This error becomes more obvious as the lateral displacement of the roll center increases significantly. This definition therefore also erroneously assumes, but does not state, that the roll center is always located at the vehicle centerline.

Neither definition is completely accurate and if taken literally, can lead to significant errors both in understanding suspension behavior, and in the results of mathematical suspension models.

In this text, the roll center will be defined in a kinematic sense by its location in the transverse plane of the wheel centers, and in a dynamic sense as a point through which tire forces act on the sprung mass.

Kinematic Location:

The roll center is located at the intersection of the two lines formed between the tire contact patches and their respective instantaneous centers (as seen in Figure 3-1). The roll center therefore moves both vertically and laterally as the instantaneous centers of each wheel move during suspension motion. Because of this dependence on suspension kinematics, the location is typically different for the front and rear suspensions.

Dynamic Effects of Roll Center Location:

- The vertical location or height of the roll center determines the resulting two moment arms formed between the roll center and both the C.G. and the ground plane. These two moment arms determine a vehicle's sensitivity to lateral acceleration by producing rollover moments and jacking forces.

- The horizontal location or lateral displacement of the roll center in conjunction with the jacking forces produce an additional rollover moment not accounted for in most texts.

- The point on the vehicle center-line at the *mean* roll center height defines the location about which the sprung mass rolls. The longitudinal axis formed between the front and rear roll centers is the roll axis. The mean point on this longitudinal axis defines the point about which the rollover moments are generated. The roll angle of the vehicle is therefore calculated at this mean roll center height on the vehicle center-line.

As described in the two items above, the roll center is the point in space in the transverse plane of the axle through which all the tire forces act (sometimes referred to as "link" forces because they act on the sprung mass through the suspension links). These "link" forces consist of vertical "jacking" forces and lateral forces. Both produce rollover moments about the roll axis. Therefore, controlling the motion of the roll center within the operational envelope of the suspension is a primary goal when designing a suspension which will be operated under large lateral accelerations.

3.13 Rollover Moment Arm - The rollover moment has three components which result from three different force and roll moment arm pairs. As seen in Figure 4-2 these rollover moment components are as follows:

- The first component is the product of the laterally accelerated sprung mass acting on the vertical roll moment arm formed between the c.g. and the roll center height (Y_{rm}). This mean rollover moment is calculated at the c.g. using the mean value of the roll moment arm. The mean rollover moment can then be distributed to the front and rear suspensions as a product of the front/rear roll resistance ratio.

- The second component is a product of the vertically accelerated sprung mass acting on the moment arm formed by the lateral displacement of the c.g. away from the center-line during roll (X_{rm}).

- The third component is a product of the jacking forces and the moment arm formed by the lateral displacement of the roll center from the vehicle center-line during roll (X_s).

The sum of these moment components causes roll during cornering. If the effects of the first rollover moment component are to be equally distributed front to rear, the front and rear vertical roll moment arms must be equal. It is beneficial therefore for the roll axis to be kept nearly parallel to the mass centroidal axis if possible. Maintaining this parallel relationship will insure that similar roll moments will be induced front and rear when the vehicle is laterally accelerated. This also helps to generate a linear diagonal load transfer during braking and cornering.

Maintaining a parallel relationship with the mass axis however, must be balanced against the need to maintain a parallel relationship between the roll axis and the ground. The ability to keep the roll axis parallel to the ground provides equal jacking forces front to rear for a given lateral acceleration. The priority of maintaining a parallel relationship with the ground or the mass axis depends on whether roll moment component #1 contributes more to load transfer for a given design than the jacking component #3. Due to the relatively low roll centers (near ground level) used in road racing, roll moment component #1 usually exceeds component #3. This compromise then is typically biased towards maintaining a parallel relationship between the roll axis and the mass axis.

Changing the kinematic relationships of the suspension components modifies the placement of the roll center, and thus the length of the three roll moment arms. Placing the roll center at the same height as the c.g. eliminates the roll moments #1 & #2 and nearly all roll. This configuration also eliminates the component of the sprung mass lateral load transfer related to roll. This design however, gives the driver little indication of load transfer and ultimately, impending traction loss. This will also increase the adverse phenomena of jacking and its contribution to roll moment.

3.14 Roll Resistance Arm - The roll resistance arm is the lever arm formed between the tread's center of pressure and the vehicle center-line (seen in Figure 3-1). This moment arm creates a roll resisting torque when acted on by the reaction forces generated at the tire contact patch by the spring and anti-roll bar. It is important to understand that this moment arm is not measured with respect to the lateral position of the roll center because the vehicle does not roll about the roll center; it rolls about the point on the center-line at the same height as the mean roll center.

3.15 Jacking - When a vehicle is laterally accelerated during cornering, the front & rear tires generate reaction forces which act on the vehicle through their respective roll centers. These tire reaction forces are transmitted to the vehicle through the suspension links. In suspensions that place the roll center above ground, the upward tire reaction force vector generated by the laden (outside) tire is greater than the downward tire reaction force vector generated by the unladen (inside) tire. When these vectors are summed, they result in a positive (upward) vertical reaction force which acts on the respective sprung mass through its roll center. This upward jacking force lifts or "jacks" the respective sprung mass upward when cornering. This upward displacement reduces negative camber angle and camber thrust. The jacking force also produces an additional rollover moment as the roll center is laterally displaced away from the vehicle centerline.

3.20 KINEMATIC OBSERVATIONS - The following is a list of observations about the kinematic response of unequal/non-parallel suspensions to certain modifications.

- Placing the static roll center at the same height as the c.g. nearly eliminates roll, but increases jacking force and its associated roll moments.

- Placing the static roll center at ground level eliminates jacking force and its rollover moment component, but increases the rollover moment's component of load transfer. This requires increased roll resistance to compensate.

- An unequal length four bar suspension is either biased towards controlling roll center motion or optimizing camber curves. This type of suspension cannot do both. The proper bias depends on external factors such as tire size, sprung mass, & track requirements, etc.

- As the upper and lower links become more parallel, the instant centers move quickly outward, decreasing lateral roll center movement in roll. Camber starts to change at the same rate and direction as vehicle roll angle. This causes the laden tire to assume a positive camber when cornering, significantly reducing adhesion.

- As the upper and lower links become more equal in length, the camber changes less in bump and droop.

- Steering axis inclination has no effect on the suspension roll center and is used primarily to compensate for the upper link geometry and reduce scrub radius.

Table 3-1 shows typical changes to roll center motion and camber control for specific design changes.

TABLE 3-1

KINEMATIC EFFECTS OF DESIGN MODIFICATIONS ON AN UNEQUAL LENGTH / NON-PARALLEL CONTROL ARM SUSPENSION

Change to baseline design in one inch increments (See Figure 6-1 for nomenclature)		CHANGE IN ROLL CENTER POSITION					CHANGE IN CAMBER SLOPE			
		During Ride Motions			During Roll		During Ride Motions		During Roll	
		Static Height	Drop during Bump	Rise during Droop	Lateral Movement	Vertical Movement	In Bump	In Droop	Left Roll	Right Roll
Changing the slope of the upper A arm	Drop Y3	>>	>	≤	<<	>>	>>>	>>>	<<	<<
	Raise Y3	<<	<	>	>>>	<<<	<<<	<<<	>>	>>
Change length of the upper arm by moving X3 the same amount	X3 In=ArmU increase	=	≥	>	≥	≤	≤	=	=	=
	X3 Out=ArmU decrease	=	≤	<	≤	≥	≥	=	=	=
Changing SAI by adjusting the upper A arm length	Increase ArmU length	=	≥	≥	≥	≤	≤	=	=	=
	Decrease ArmU length	=	≤	<	≤	≥	≥	=	=	=
Changing the slope of the lower A arm	Drop Y2	<<<	<<<	<<<	<<	<<<	>>>	<<<	>>	>>
	Raise Y2	>>>	>>>	>	>>	>>>	<<<	>>>	<<	<<
Change length of the lower arm by moving X2 the same amount	X2 In=ArmL increase	≤	<<	<<	<	>	=	=	=	=
	X2 Out=ArmL decrease	≥	>>	>>>	>	<	=	=	=	=
Changing SAI by adjusting the lower A arm length	Increase ArmL length	≤	=	<<	≤	>	≥	=	=	=
	Decrease ArmL length	≥	=	>>	≥	<	≤	=	=	=
Changing the slope of the upper & lower A arms equally	Raise Y2 & Y3 equally	<<<	<<<	<	<<	<<	>	>	<	<
	Lower Y2 & Y3 equally	>>>	>>>	>	>>	>>	<	<	>	>

Legend: <: Reduction in roll center height, lateral displacement, or camber angle change

>: Increase in roll center height, lateral displacement, or camber angle change

= no significant change ≤ or ≥ very small change < or > small change << or >> large change <<< or >>> very large change

For Example: Dropping Y3 causes:

1) A large increase in the static roll center height
2) An increase in the drop of the roll center during bump
3) A very small decrease in the rise of the roll center during droop
4) A large reduction in lateral movement of the roll center away from the centerline during roll
5) A large drop of the roll center as it moves away from the centerline during roll
6) Very large increases in camber angle during both bump and droop
7) A large reduction in camber angle during left & right roll

Note: These observations are highly dependent on the link lengths and angular relationships which existed in the baseline design. Therefore, they may not represent the results which may be produced by similar modifications on another design. Use the above trends as a general guide during the optimization process and note any deviations.

IV VEHICLE DYNAMICS

The motive forces which a tire can generate depend to a certain extent on the vertical load which is forcing the bond with the road surface. Controlling the levels of this load within the optimum levels of the tire design and the fluctuations of this load during transient motions of the vehicle is accomplished both by smooth driving techniques and proper suspension design.

4.10 MASS PROPERTIES - Many factors are involved in the transfer of load within an accelerating vehicle. The first obviously is mass. The more the vehicle weighs, the more load will be transferred for any given acceleration. Mass in a vehicle is categorized into two types, sprung and unsprung. Sprung mass is the mass of the vehicle which is supported by the suspension springs, and unsprung mass is all other mass such as wheels and tires.

4.11 Center of Gravity - The first characteristic of mass is its center of gravity. The c.g. is the point in three dimensional space from which the vehicle can be suspended and maintain equilibrium. All accelerative forces (not tire or "link" forces which act on the roll center) act on the vehicle through this point. Therefore, the lower the center of gravity, the less load will be transferred either longitudinally from rear to front when braking, or laterally from side to side when cornering. Related to the center of gravity, is the mass centroid axis. This is the c.g. of each section of the vehicle if the vehicle were to be divided up into sections along the longitudinal axis (as seen in Figure 4-1).

4.12 Moments of Inertia - The second characteristic of mass is its distribution away from the c.g. Any mass distributed away from the c.g. creates a moment of inertia. These moments exist in the planes of roll (longitudinal), yaw (vertical), and pitch (lateral). The greater the mass is located away from the c.g., the more acceleration will affect load transfers in any of these planes.

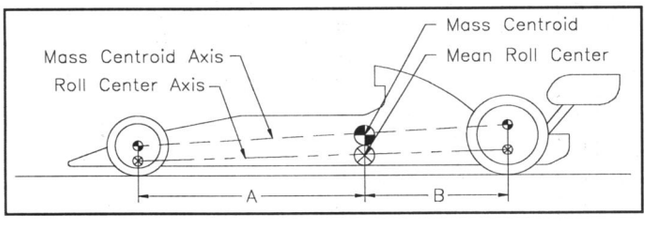

FIGURE 4-1

MASS CENTROID AXIS
RELATIVE TO ROLL CENTER AXIS

4.20 CHANGES IN ATTITUDE - Large forces are generated when the sprung and unsprung masses are accelerated. These masses are accelerated vertically during bump and droop, laterally during cornering, and longitudinally during braking or acceleration. These accelerations cause changes in vehicle attitude and load transfer. Lateral acceleration during cornering causes the vehicle to roll and possibly yaw. Longitudinal acceleration during acceleration or braking causes the vehicle to pitch. Vertical acceleration during bump or droop may also cause the vehicle to pitch.

4.30 LOAD TRANSFER - Tire load is increased or decreased (transferred) when the sprung and unsprung masses are acted upon by these external accelerations. Load is transferred from the inside (unladen) to the outside (laden) tires during cornering; from the front to the rear during acceleration, and from the rear to the front during braking. Tire load is increased during bump, and decreased during droop. The analysis becomes more complex when these accelerations are combined. For example, load is transferred to the outside front tire during turn entry when the brakes are applied. Managing these load transfers is of great importance if the vehicle is to be controllable and stable. The linearity of the transfer curves can be as important as the total load transferred. The worst thing for the driver to experience is a significant non linearity in load transfer and adhesion at a time when he or she is not expecting it.

4.31 Lateral Load Transfer Due to Sprung Mass - Sprung mass load transfer can be analyzed by the following two mechanisms (seen in Figure 4.2):

A) The first mechanism of sprung mass lateral load transfer is the mean rollover moment which the sprung mass produces about the mean roll center when laterally accelerated. The mean rollover moment is made up of the three components discussed in section 3.13.

B) The second mechanism is the non-rollover moment which the sprung mass produces about the ground plane when laterally accelerated. This torque can only be calculated once the sprung mass is transferred (along with the accompanying mean rollover moment) to the mean point on the center-line at the same height as the mean roll center. **Note:** this is simply a matter of transferring a force and mass to a different point in space by applying the required torque about the new location.

The sprung mass and mean rollover moment is then distributed from this location to the point on the center-line at the respective front and rear roll center heights as a product of the front/rear roll resistance ratio. Once these are distributed, the contribution of this second mechanism can be quantified for the front and rear suspensions.

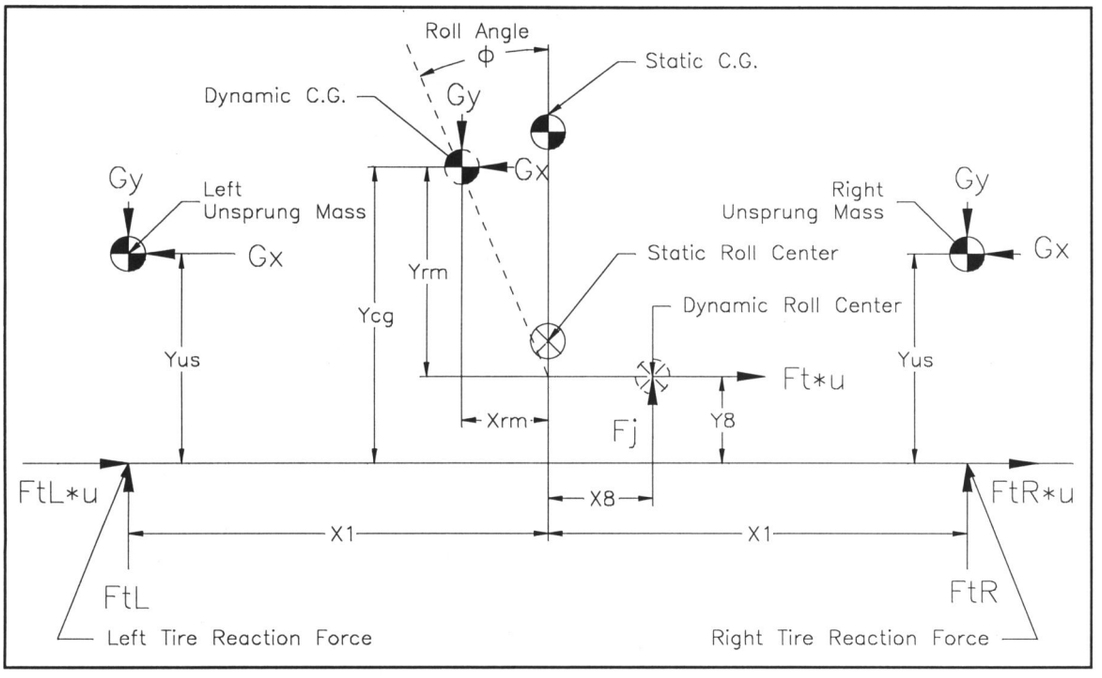

FIGURE 4-2

LATERAL LOAD TRANSFER PARAMETERS

4.32 Lateral Load Transfer Due to Unsprung Mass - Load is transferred by the unsprung mass through the following two mechanisms (seen in Figure 4.2):

A) The first mechanism of unsprung mass lateral load transfer is due to the moment which the unsprung mass produces about the ground. When laterally accelerated, the unsprung mass acts on the moment arm formed between the unsprung c.g. and the ground.

B) The second mechanism is due to the camber change of the tire/wheel assembly. As the tire rolls, the c.g. moves laterally away from the contact patch center of pressure. This lateral displacement forms a moment arm. The unsprung mass produces an additional moment about this arm when vertically accelerated. Due to the small angles of camber seen in road racing however, this contribution to load transfer is typically ignored.

4.33 Longitudinal Load Transfer Due to Sprung Mass - Load is transferred longitudinally when pitching moments are generated about the longitudinal center of the vehicle. This pitching moment can be created when braking & accelerating, and during bump & droop.

A) During braking or acceleration, the longitudinal acceleration acts on the sprung & unsprung masses to create a pitching moment about the ground plane. This pitching moment transfers load from one end of the vehicle to the other.

B) In vehicles which do not have an equal static weight distribution front to rear, the c.g. is located either forward or rearward of the longitudinal center of the vehicle. When this type of vehicle is vertically accelerated, additional pitching moments are generated about the longitudinal center of the vehicle. For example, in vehicles with a rear weight bias, downward acceleration in bump will cause load to transfer to the rear, and vice-versa.

V SUSPENSION DESIGN RECOMMENDATIONS

The following is a list of design recommendations listed in order of priority, which should provide a good starting point in the modeling/design of an unequal length control arm suspension.

1) Use the longest lower control link possible to minimize camber change.
2) A low roll center should used be to reduce jacking and camber change. This will also provide the driver with a linear feeling of load transfer while minimizing the chance of traction loss. Static roll centers are usually placed near ground level.
3) Reduce roll center motion during roll. This will reduce the contribution that the lateral displacement makes to rollover moment. It will also help maintain a constant relationship with the mass centroid axis.
4) Front camber change during roll should have a slight negative slope. This assures adequate contact patch area and camber thrust. This also reduces understeer of the front laden tire during turn entry.

5) Minimize toe change during bump (bump steer).

6) The roll axis should have a similar slope to the mass centroid axis. This will provide linear diagonal load transfer during cornering.

7) Minimize track width change during ride and roll changes.

8) The motion ratio should be kept near 1.0 to improve damper/spring efficiency.

9) Use linear rising wheel rates (greater than 15% rising rate usually requires an inboard suspension design).

10) Minimize scrub radius. SAI angles up to 10 degrees are common.

11) Be careful when using anti-dive geometry due to its effects on caster during travel.

VI DEVELOPING A MATHEMATICAL MODEL

Considering the complex constraints and the number of variables under consideration, suspensions can be effectively modeled only on computers. This section describes the process of developing a simple two dimensional steady-state kinematic and dynamic model for an unequal length four bar link suspension system commonly found in competition vehicles.

This is a steady-state model which ignores time based factors such as: damping, rates of change and response. The intent of this model is to provide the reader with simple non-differential mathematical equations in the hope that these can be used for an understanding of the basic principles of motion and load transfer.

A more extensive model would consider the effects of time and the third plane of action. This type of model was considered overly complex for the basic understanding this text attempts to provide.

These equations cover suspension motions in two dimensions (vertical and lateral), due to bump, droop and roll. Effects of caster, and other longitudinal geometrical constraints are not considered. These effects however can easily be added. Load transfer in two planes (lateral and longitudinal), due to bump, droop, roll and pitch is covered along with tire load changes due to bump and droop. Load transfer due to yaw is also not covered.

6.10 2D STEADY-STATE KINEMATIC MODELING EQUATIONS - The 2D Kinematic Model Diagram seen in Figure 6-1 will be used to develop the equations which model the kinematic motions of the suspension. The kinematic modeling variables in this diagram are defined using the equations on the following pages.

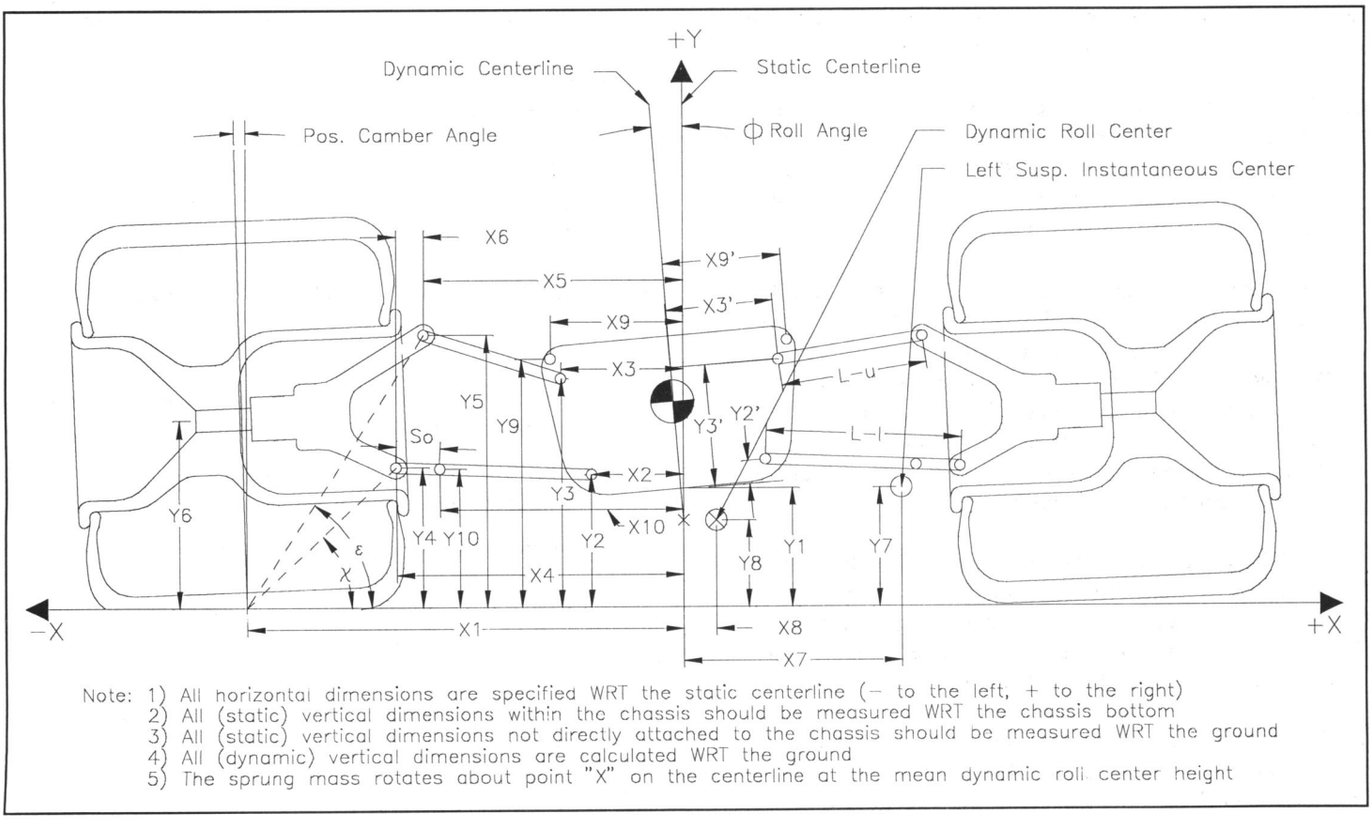

FIGURE 6-1

2D KINEMATIC MODELING PARAMETERS

NOTE: Unless otherwise stated, left and right versions of the following equations are equivalent once the subscripts are changed from left to right. The following equations ignore tire compliance.

X_{1L} & X_{1R} = 1/2 the **absolute value** of the track width

$$X_{1L} = Track'/2 + \left(X'_{4L} - X_{4L}\right) + \left(\cos\chi_L - \cos\chi'\right)\sqrt{Y_4'^2 + \left(X'_1 - \left|X'_{4L}\right|\right)^2} \quad \text{(EQ 6-1)}$$

$$X_{1R} = Track'/2 + \left(X_{4R} - X'_{4R}\right) + \left(\cos\chi_R - \cos\chi'\right)\sqrt{Y_4'^2 + \left(X'_1 - \left|X'_{4R}\right|\right)^2} \quad \text{(EQ 6-1A)}$$

X_1 = Average of the left & right absolute track widths

$$X_1 = \frac{X_{1L} + X_{1R}}{2} \quad \text{(EQ 6-2)}$$

where "X'" and "Y'" are the static values of each dimension, "X_L" & "X_R" are the left and right values of each dimension respectively.

Y_{1f} = Front ground clearance (rear is similar)

$$Y_{1f} = Y'_{1f} - \frac{\left(G_y - 1g\right)M_{sf} + LT_z - F_{jf}}{2K_{sf}\,MR_{sf}^{\,2}} + \left(\left(\frac{\sin\chi_L + \sin\chi_R}{2}\right) - \sin\chi'\right)\sqrt{Y_4'^2 + \left(X'_1 - \left|X'_4\right|\right)^2} \quad \text{(EQ 6-3)}$$

In this equation, "G_y" is the vertical acceleration in "G's", "$1g$" is the acceleration due to gravity in "G's", "M_{sf}" is the front sprung mass, "F_{jf}" is the front jacking force, "LT_z" is the longitudinal load transfer, "K_{sf}" is the front spring rate, and "MR_{sf}" is the front motion ratio for the springs.

The third term in the ride height equation is the reduction in ride height due to the drop of the lower kingpin ball joint as the wheel changes camber. The chassis drops by the same amount as the drop in the lower ball joint in suspensions supported by springs which act on the lower control arm. **Note:** The third term in this equation should be changed to account for the drop in the upper kingpin ball joint in suspensions which are sprung by the upper control arm. Rear ground clearance is calculated in the same manner.

χ' & χ = The static and instantaneous angle which the imaginary line between the lower kingpin ball joint and the center of the tire contact patch makes with the ground is found by (EQ 6-4) & (EQ 6-5):

$$\chi' = \arctan\left(\frac{Y'_4}{X'_1 - \left|X'_4\right|}\right) \quad \text{(EQ 6-4)}$$

$$\chi = \chi' + \left(\theta - \theta'\right) = \arctan\left(\frac{Y'_4}{X'_1 - \left|X'_4\right|}\right) + \left(\theta - \theta'\right) \quad \text{(EQ 6-5)}$$

where "θ" is wheel camber.

X_2 & Y_2 = Lower inner pick up point (left shown, right is similar)

$$X_{2L} = X'_{2L}\cos\phi + Y'_2\sin\phi + \left(Y_1 - Y_8\right)\tan\phi \quad \text{(EQ 6-6)}$$

$$Y_{2L} = Y_1 + Y'_2\cos\phi - X'_{2L}\sin\phi \quad \text{(EQ 6-7)}$$

where "ϕ" is the roll angle of the sprung mass.

X_3 & Y_3 = Upper inner pick up point (left shown, right is similar)

$$X_{3L} = X'_{3L}\cos\phi + Y'_3\sin\phi + \left(Y_1 - Y_8\right)\tan\phi \quad \text{(EQ 6-8)}$$

$$Y_{3L} = Y_1 + Y'_3\cos\phi - X'_{3L}\sin\phi \quad \text{(EQ 6-9)}$$

The equations for the upper & lower inner pick up points consider the fact that the vehicle rolls about a point on the centerline at the mean dynamic roll center height.

X_4 & Y_4 = Lower hub carrier pick up point ("Y_{4L}" is shown, "Y_{4R}" is similar)

$$X_{4L} = X_{2L} - \sqrt{L_l^{\,2} - \left(Y_{4L} - Y_{2L}\right)^2} \quad \text{(EQ 6-10)}$$

$$X_{4R} = X_{2R} + \sqrt{L_l^{\,2} - \left(Y_{4R} - Y_{2R}\right)^2} \quad \text{(EQ 6-10A)}$$

$$Y_{4L} = Y'_4 + \left(\sin\chi_L - \sin\chi'\right)\sqrt{Y_4'^2 + \left(X'_1 - \left|X'_{4L}\right|\right)^2} \quad \text{(EQ 6-11)}$$

(when vehicle is not airborne)

$$Y_{4L} = Y'_4 + \left(\sin\chi_L - \sin\chi'\right)\sqrt{Y_4'^2 + \left(X'_1 - \left|X'_{4L}\right|\right)^2} + Y_1 - \left(Y'_1 + D_m\right) \quad \text{(EQ 6-11A)}$$

(when vehicle becomes airborne)

In equations 6-10 & 6-11, "L_l" is the lower control arm length, and "D_m" is the maximum suspension droop. The second term in the equations for "Y_4" is the change in the height of the lower kingpin ball joint due to changes in wheel camber.

X_5&Y_5= Upper hub carrier pick up point ("Y_{5L}" is shown, "Y_{5R}" is similar)

$$X_{5L} = X_{3L} - \sqrt{L_u{}^2 - (Y_{5L} - Y_{3L})^2} \quad \text{(EQ 6-12)}$$

$$X_{5R} = X_{3R} + \sqrt{L_u{}^2 - (Y_{5R} - Y_{3R})^2} \quad \text{(EQ 6-12A)}$$

$$Y'_{5L} = Y'_4 + H_{hc} \quad \text{(EQ 6-13)}$$

$$Y_{5L} = Y'_5 + (\sin\varepsilon_L - \sin\varepsilon')\sqrt{Y'^2_5 + (X'_1 - |X'_{5L}|)^2} \quad \text{(EQ 6-14)}$$

(when vehicle is not airborne)

$$Y_{5L} = Y'_5 + (\sin\varepsilon_L - \sin\varepsilon')\sqrt{Y'^2_5 + (X'_1 - |X'_{5L}|)^2} + Y_1 - (Y'_1 + D_m) \quad \text{(EQ 6-14A)}$$

(when vehicle becomes airborne)

In equations 6-12 & 6-14, "L_u" is the upper control arm length, and "H_{hc}" is the hub carrier height. The second term in the equations for "Y_5" is the change in the height of the upper kingpin ball joint due to changes in wheel camber.

ε'&ε= The static and instantaneous angle which the imaginary line between the upper kingpin ball joint and the center of the tire contact patch makes with the ground is found by (EQ 6-15) & (EQ 6-16):

$$\varepsilon' = \arctan\left(\frac{Y'_5}{X'_1 - |X'_5|}\right) \quad \text{(EQ 6-15)}$$

$$\varepsilon = \varepsilon' + (\theta - \theta') = \arctan\left(\frac{Y'_5}{X'_1 - |X'_5|}\right) + (\theta - \theta') \quad \text{(EQ 6-16)}$$

X_6= Hub carrier offset (left shown, right is similar)

$$X_{6L} = X_{5L} - X_{4L} \quad \text{(EQ 6-17)}$$

Y_6= Spindle height

$$Y_6 = Y'_6 \quad \text{(EQ 6-18)}$$

(when vehicle is not airborne)

$$Y_6 = Y'_6 + Y_1 - (Y'_1 + D_m) \quad \text{(EQ 6-18A)}$$

(when vehicle becomes airborne)

SAI'= Static Steering Axis Inclination

$$SAI' = \arctan\left(\frac{X'_{4R} - X'_{5R}}{Y'_5 - Y'_4}\right) \quad \text{(EQ 6-19)}$$

"θ "= Wheel camber

$$\theta_L = SAI' + \arctan\left(\frac{X_{4L} - X_{5L}}{Y_{5L} - Y_{4L}}\right) \quad \text{(EQ 6-20)}$$

$$\theta_R = SAI' - \arctan\left(\frac{X_{4R} - X_{5R}}{Y_{5R} - Y_{4R}}\right) \quad \text{(EQ 6-20A)}$$

$Scrub$ = Scrub Radius (left shown, right is similar)

$$Scrub_L = X_{1L} - \left(Y_{4L}\tan(SAI' - (\theta - \theta')) + X_{4L}\right) \quad \text{(EQ 6-21)}$$

X_7&Y_7= Instantaneous Center (left shown, right is similar)

$$X_{7L} = \frac{\left(Y_{2L} - X_{2L}\left(\frac{Y_{4L} - Y_{2L}}{X_{4L} - X_{2L}}\right)\right) - \left(Y_{3L} - X_{3L}\left(\frac{Y_{5L} - Y_{3L}}{X_{5L} - X_{3L}}\right)\right)}{\left(\frac{Y_{5L} - Y_{3L}}{X_{5L} - X_{3L}}\right) - \left(\frac{Y_{4L} - Y_{2L}}{X_{4L} - X_{2L}}\right)} \quad \text{(EQ 6-22)}$$

$$Y_{7L} = \left(\frac{Y_{5L} - Y_{3L}}{X_{5L} - X_{3L}}\right)(X_{7L} - X_{3L}) + Y_{3L} \quad \text{(EQ 6-23)}$$

The location of the instantaneous center (see Figure 3-1) is calculated by finding the intersection of the upper and lower control arm extensions. This intersection is found by setting the equation ($Y = mX + b$) for the upper & lower control arms equal to each other.

X_8&Y_8= Roll Center

$$X_8 = X_1\left(\frac{Y_{7L}(X_{7R} - X_{1R}) - Y_{7R}(-X_{7L} - X_{1L})}{-Y_{7L}(X_{7R} - X_{1R}) - Y_{7R}(-X_{7L} - X_{1L})}\right) \quad \text{(EQ 6-24)}$$

$$Y_8 = \frac{-Y_{7L}(X_8 + X_1)}{-X_{7L} - X_1} \quad \text{(EQ 6-25)}$$

where "X_{7L}&Y_{7L}" & "X_{7R}&Y_{7R}" are the left and right values respectively.

The location of the roll center (see Figure 3-1) is calculated by finding the intersection of the vectors which connect the instantaneous centers with their respective tire contact patches. This intersection is found using the same methods used in EQ 6-22 & 6-23.

$X_9 \& Y_9$= Upper Outboard Spring/Damper pick up point (left shown, right is similar)

$$X_{9L} = X'_{9L}\cos\phi + Y'_9\sin\phi + (Y_1 - Y_8)\tan\phi \qquad \text{(EQ 6-26)}$$

$$Y_{9L} = Y_1 + Y'_9\cos\phi - X'_{9L}\sin\phi \qquad \text{(EQ 6-27)}$$

$X_{10} \& Y_{10}$= Lower Outboard Spring/Damper or push-rod pick up point

$$X_{10L} = X_{2L} - (L_l - S_o)\cos\left(\arctan\left(\frac{Y_{4L} - Y_{2L}}{-(X_{4L} - X_{2L})}\right)\right) \qquad \text{(EQ 6-28)}$$

$$X_{10R} = X_{2R} + (L_l - S_o)\cos\left(\arctan\left(\frac{Y_{4R} - Y_{2R}}{X_{4R} - X_{2R}}\right)\right) \qquad \text{(EQ 6-28A)}$$

$$Y_{10L} = Y_{2L} + (L_l - S_o)\sin\left(\arctan\left(\frac{Y_{4L} - Y_{2L}}{-(X_{4L} - X_{2L})}\right)\right) \qquad \text{(EQ 6-29)}$$

$$Y_{10R} = Y_{2R} + (L_l - S_o)\sin\left(\arctan\left(\frac{Y_{4R} - Y_{2R}}{X_{4R} - X_{2R}}\right)\right) \qquad \text{(EQ 6-29A)}$$

where "S_o" is the offset of the lower spring/damper or push-rod pick up from the lower kingpin pick up point. **Note:** this formula assumes that the lower spring/damper or push-rod pick up point is in-line with the lower control arm.

$S'_{IL} \& S_{IL}$= Static & instantaneous length of Outboard Spring/Damper unit (left shown, right is similar)

$$S'_{IL} = \sqrt{(X'_{10L} - X'_{9L})^2 + (Y'_{9L} - Y'_{10L})^2} \qquad \text{(EQ 6-30)}$$

$$S_{IL} = \sqrt{(X_{10L} - X_{9L})^2 + (Y_{9L} - Y_{10L})^2} \qquad \text{(EQ 6-31)}$$

δ_s= Spring Deflection

$$\delta_s = S_l - S'_l \qquad \text{(EQ 6-32)}$$

$X_{11} \& Y_{11}$= Upper Pull-rod pick up point (only used on pull-rod suspension types discussed later)

$$X_{11L} = X_{3L} - (L_u - P_o)\cos\left(\arctan\left(\frac{Y_{5L} - Y_{3L}}{-(X_{5L} - X_{3L})}\right)\right) \qquad \text{(EQ 6-33)}$$

$$X_{11R} = X_{3R} + (L_u - P_o)\cos\left(\arctan\left(\frac{Y_{5R} - Y_{3R}}{X_{5R} - X_{3R}}\right)\right) \qquad \text{(EQ 6-33A)}$$

$$Y_{11L} = Y_{3L} + (L_u - P_o)\sin\left(\arctan\left(\frac{Y_{5L} - Y_{3L}}{-(X_{5L} - X_{3L})}\right)\right) \qquad \text{(EQ 6-34)}$$

$$Y_{11R} = Y_{3R} + (L_u - P_o)\sin\left(\arctan\left(\frac{Y_{5R} - Y_{3R}}{X_{5R} - X_{3R}}\right)\right) \qquad \text{(EQ 6-34A)}$$

where "P_o" is the offset of the upper pull-rod pick up from the upper kingpin pick up point. **Note:** this formula also assumes that the upper pull-rod pick up point is in-line with the upper control arm.

$X_{12} \& Y_{12}$= Push or Pull-rod bell-crank pivot point (used only in inboard suspensions discussed later) (left shown, right is similar)

$$X_{12L} = X'_{12L}\cos\phi + Y'_{12}\sin\phi + (Y_1 - Y_8)\tan\phi \qquad \text{(EQ 6-35)}$$

$$Y_{12L} = Y_1 + Y'_{12}\cos\phi - X'_{12L}\sin\phi \qquad \text{(EQ 6-36)}$$

The inboard spring mounting point "$X_{14} \& Y_{14}$" used in inboard suspensions can be calculated by using (EQ 6-35 &36) and substituting "$X'_{14} \& Y'_{14}$" for "$X'_{12} \& Y'_{12}$".

6.20 2D DYNAMIC MODELING EQUATIONS

6.21 Lateral Load Transfer - Figure 4-2 describes the nomenclature which will be used to develop this model.

The process of calculating the lateral load transfer consists of the following five steps:

Step #1 - The first step is to calculate the mean rollover moment of the sprung mass. This moment has three components (described in section 3.13). The rollover moment is calculated using the c.g height, and the mean values of roll center height and track width. These mean values are defined by the longitudinal location of the c.g. along the vehicle's centerline (seen in Figure 6-2).

The height of the center of gravity can be calculated using (EQ 6-37):

$$Y_{c.g.} = \frac{(Y_{c.g.r}A) + (Y_{c.g.f}B)}{A + B} \qquad \text{(EQ 6-37)}$$

where "$Y_{c.g.f}$" & "$Y_{c.g.r}$" are the front and rear c.g. heights respectively.

The mean roll center Y_{8m} can then be calculated using (EQ 6-38):

$$Y_{8m} = \frac{(Y_{8r}A) + (Y_{8f}B)}{A + B} \qquad \text{(EQ 6-38)}$$

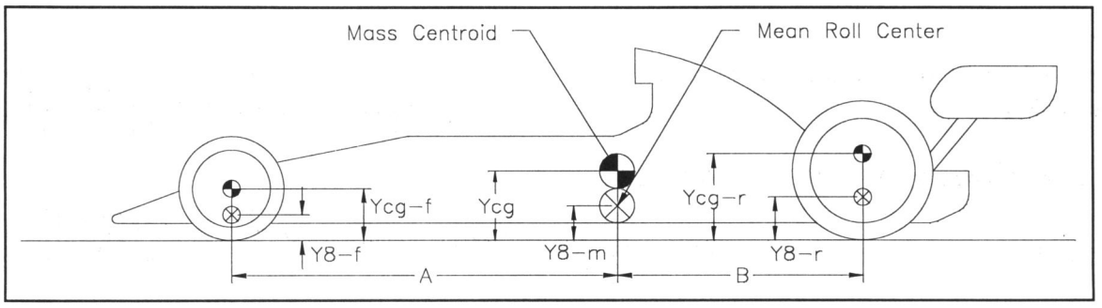

FIGURE 6-2

MEAN LOCATION OF ROLL CENTER

The mean 1/2 track X_{1m} is found using EQ (6-39):

$$X_{1m} = \frac{(X_{1r}A)+(X_{1f}B)}{A+B} \qquad \text{(EQ 6-39)}$$

where A is the longitudinal distance from the c.g. to the front axle, and B is the longitudinal distance from the c.g. to the rear axle.

Once these mean values are known, the moment about the point on the centerline at the mean roll center height (as seen in Figure 6-3) can be calculated using (EQ 6-40) (CW=+):

$$\sum M = 0 = F_{tL}X_{1m} - F_{tR}X_{1m} - M_s G_x (Y_{c.g.} - Y_{8m}) - M_s G_y \tan\phi (Y_{c.g.} - Y_{8m}) - F_{jt}X_{8m} \qquad \text{(EQ 6-40)}$$

In EQ 6-40, "F_{tL}" & "F_{tR}" are the left and right tire reaction forces, "M_s" is the sprung mass, "G_x" & "G_y" are the lateral and vertical accelerations in G's, and "F_{jt}" is the total front & rear jacking force.

The resulting mean rollover moment can then be found using (EQ 6-41) (CW=+)

$$ROM = -M_s G_x (Y_{c.g.} - Y_{8m}) - M_s G_y \tan\phi (Y_{c.g.} - Y_{8m}) - F_{jt}X_{8m} \qquad \text{(EQ 6-41)}$$

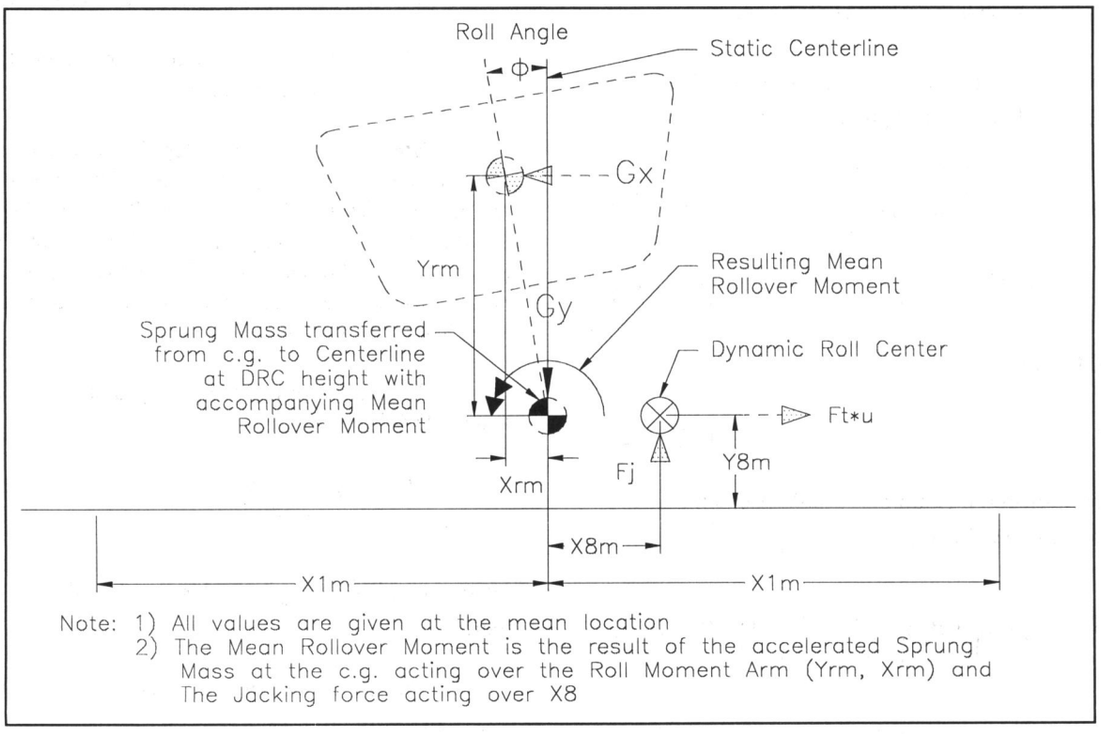

FIGURE 6-3

MEAN ROLLOVER MOMENT DIAGRAM

Step #2 - The second step is to calculate the mean sprung mass load transferred from the inner two tires to the outer two tires using the known mean rollover moment. This is accomplished by simultaneously solving for the left and right tire reaction forces F_{tL} and F_{tR} using (EQ 6-42) and (EQ 6-43); and summing vertical forces to zero: $M_s G_y = F_{tL} + F_{tR}$.

$$F_{tL} = \frac{M_s G_y}{2} + \frac{M_s\left(Y_{c.g.} - Y_{8m}\right)\left(G_x + G_y \tan\phi\right) + F_{jt} X_{8m}}{2X_{1m}} \quad \text{(EQ 6-42)}$$

$$F_{tR} = \frac{M_s G_y}{2} - \frac{M_s\left(Y_{c.g.} - Y_{8m}\right)\left(G_x + G_y \tan\phi\right) - F_{jt} X_{8m}}{2X_{1m}} \quad \text{(EQ 6-43)}$$

The resulting sprung mass load transferred from the unladen to laden tires due to the mean rollover moment is therefore defined by (EQ 6-44):

$$LT_{1m} = \frac{F_{tL} - F_{tR}}{2} = \frac{M_s\left(G_x\left(Y_{c.g.} - Y_{8m}\right) + G_y \tan\phi\left(Y_{c.g.} - Y_{8m}\right)\right) + F_{jt} X_{8m}}{2X_{1m}} \quad \text{(EQ 6-44)}$$

Step #3 - The front and rear load transfers due to the roll moment can now be calculated as a product of the mean load transfer (step #2) and the ratio of front to rear roll resistance. (EQ 6-44) cannot be used to directly calculate the front or rear load transfer due to the roll moment because the roll resistance of each suspension determines the percent of the mean roll moment that is distributed to the each end of the vehicle. This only applies for a torsionally stiff chassis. The front LT_{1f} and rear LT_{1r} load transfers are then calculated by equations (EQ 6-45) and (EQ 6-46) respectively.

$$LT_{1f} = \left(\frac{RR_f}{RR_t}\right)\left(\frac{F_{tL} - F_{tR}}{2}\right) = \left(\frac{RR_f}{RR_t}\right)\left(\frac{M_s\left(G_x\left(Y_{c.g.} - Y_{8m}\right) + G_y \tan\phi\left(Y_{c.g.} - Y_{8m}\right)\right) + F_{jt} X_{8m}}{2X_{1m}}\right) \quad \text{(EQ 6-45)}$$

$$LT_{1r} = \left(\frac{RR_r}{RR_t}\right)\left(\frac{F_{tL} - F_{tR}}{2}\right) = \left(\frac{RR_r}{RR_t}\right)\left(\frac{M_s\left(G_x\left(Y_{c.g.} - Y_{8m}\right) + G_y \tan\phi\left(Y_{c.g.} - Y_{8m}\right)\right) + F_{jt} X_{8m}}{2X_{1m}}\right) \quad \text{(EQ 6-46)}$$

RR_f, RR_r and RR_t are defined as the front, rear and total roll resistance of the vehicle (see EQ 6-65). The resulting front rollover moment diagram is shown in Fig. 6-4.

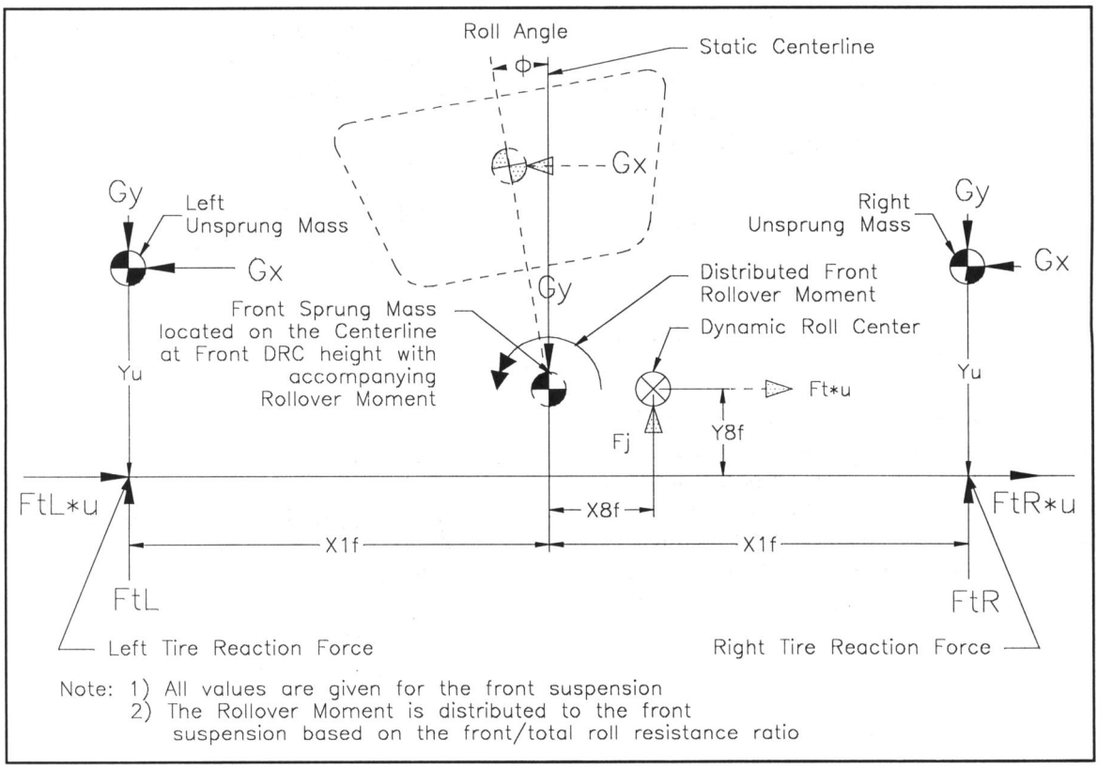

FIGURE 6-4

DISTRIBUTED (FRONT) ROLLOVER MOMENT DIAGRAM

Step #4 - The fourth step is to calculate the sprung mass load transfer due to the non-rollover moment. This moment is created when the sprung mass at each end of the vehicle is laterally accelerated over the moment arm formed between the roll center and ground. **Note:** The sprung mass of the respective suspension and the accompanying rollover moment are now located at the point on the vehicle center-line at the height of their respective roll center. We have already calculated the load transfer due to the rollover moment and are now only concerned with the effects which the sprung mass (which has been transferred to the point on the center-line at the roll center height) has on the load transfer(described in section 4.31.B).

The moment equation (front shown) of the sprung mass about the ground is calculated by (EQ 6-47) (CW=+):

$$\sum M = 0 = F_{t2L} X_{1f} - F_{t2R} X_{1f} - M_{sf} G_x Y_{8f} \qquad \text{(EQ 6-47)}$$

The second component of the tire reaction forces F_{t2L} and F_{t2R} are then solved simultaneously by summing vertical forces equal to zero: $M_{sf} G_y = F_{t2L} + F_{t2R}$. The vertical force (for the front suspension) on the left and right tires from the non-roll moment is given by (EQ 6-48) and (EQ 6-49):

$$F_{t2L} = \frac{M_{sf} G_y}{2} + \frac{M_{sf} G_x Y_{8f}}{2X_{1f}} \qquad \text{(EQ 6-48)}$$

$$F_{t2R} = \frac{M_{sf} G_y}{2} - \frac{M_{sf} G_x Y_{8f}}{2X_{1f}} \qquad \text{(EQ 6-49)}$$

Therefore, the sprung mass load transferred from the unladen to laden tires due to the non-roll moment is defined for the front and rear by (EQ 6-50) and (EQ 6-51):

$$LT_{2f} = \frac{F_{t2L} - F_{t2R}}{2} = \frac{M_{sf} G_x Y_{8f}}{2X_{1f}} \qquad \text{(EQ 6-50)}$$

$$LT_{2r} = \frac{F_{t2L} - F_{t2R}}{2} = \frac{M_{sr} G_x Y_{8r}}{2X_{1r}} \qquad \text{(EQ 6-51)}$$

Step #5 - The final step in calculating the lateral load transfer is to determine the unsprung mass load transfer. This load transfer is generated when the unsprung mass is accelerated over the moment arm formed between the c.g. of the unsprung mass (Y_u) and the ground. **Note:** the moment arm created by increasing camber angle will be ignored here. The equations are similar to those of the non-rollover moment sprung mass transfer.

The moment equation (front suspension shown) of the unsprung mass about the ground is calculated using (EQ 6-52) (CW=+):

$$\sum M = 0 = F_{t3L} X_{1f} - F_{t3R} X_{1f} - M_{uf} G_x Y_{uf} \qquad \text{(EQ 6-52)}$$

The third component of the tire reaction forces F_{t3L} and F_{t3R} are then solved simultaneously by summing vertical forces equal to zero: $M_{uf} G_y = F_{t3L} + F_{t3R}$. The vertical force (for the front suspension) on the left and right tires from the unsprung mass is defined by (EQ 6-53) and (EQ 6-54):

$$F_{t3L} = \frac{M_{uf} G_y}{2} + \frac{M_{uf} G_x Y_{uf}}{2X_{1f}} \qquad \text{(EQ 6-53)}$$

$$F_{t3R} = \frac{M_{uf} G_y}{2} - \frac{M_{uf} G_x Y_{uf}}{2X_{1f}} \qquad \text{(EQ 6-54)}$$

Therefore, the unsprung mass load transferred from the unladen to laden tires is defined for the front and rear by (EQ 6-55 and (EQ 6-56):

$$LT_{3f} = \frac{F_{t3L} - F_{t3R}}{2} = \frac{M_{uf} G_x Y_{uf}}{2X_{1f}} \qquad \text{(EQ 6-55)}$$

$$LT_{3r} = \frac{F_{t3L} - F_{t3R}}{2} = \frac{M_{ur} G_x Y_{ur}}{2X_{1r}} \qquad \text{(EQ 6-56)}$$

The total lateral load transferred due to lateral and vertical accelerations for the front and rear suspensions is then found by (EQ 6-57) and (EQ 6-58)

$$LT_{tf} = LT_{1f} + LT_{2f} + LT_{3f} = \left(\frac{RR_f}{RR_t}\right)\left(\frac{M_s\left(G_x\left(Y_{c.g.} - Y_{8m}\right) + G_y \tan\phi\left(Y_{c.g.} - Y_{8m}\right)\right) + F_{jt} X_{8m}}{2X_{1m}}\right) + \frac{M_{sf} G_x Y_{8f}}{2X_{1f}} + \frac{M_{uf} G_x Y_{uf}}{2X_{1f}} \qquad \text{(EQ 6-57)}$$

$$LT_{tr} = LT_{1r} + LT_{2r} + LT_{3r} = \left(\frac{RR_r}{RR_t}\right)\left(\frac{M_s\left(G_x\left(Y_{c.g.} - Y_{8m}\right) + G_y \tan\phi\left(Y_{c.g.} - Y_{8m}\right)\right) + F_{jt} X_{8m}}{2X_{1m}}\right) + \frac{M_{sr} G_x Y_{8r}}{2X_{1r}} + \frac{M_{ur} G_x Y_{ur}}{2X_{1r}} \qquad \text{(EQ 6-58)}$$

6.22 Roll Resistance - The roll moment generated when the sprung mass is laterally accelerated must be resisted to maintain stability. This resisting couple (as seen in Figure 6-5) is generated through the tire contact patches by the springs and anti-roll bars. These tire forces form a couple around the vehicle center-line which limits the roll angle for a given lateral acceleration. Roll resistance and its distribution therefore affects the entire suspension design. For example, the load transferred from the inner rear tire to the outer front tire at turn entry has a large effect on the acceptable levels of camber and roll center movements. The suspension design process requires both experience and many iterations of the model to obtain the required balance.

Using Figure 6-5, the roll resistance couple RRC_f (front suspension shown) is found to be (EQ 6-59):

$$RRC_f = F_{tL} X_{1f} - F_{tR} X_{1f} \qquad \text{(EQ 6-59)}$$

where the left and right total tire reaction forces F_{tL} and F_{tR} are calculated using (EQ 6-60) and (EQ 6-61):

$$\begin{aligned} F_{tL} &= F_{ts} + \delta_{wfL} K_{wfL} \\ &= F_{ts} + \sin\phi\left(X_{1f} + \tan\phi\left(Y_{6f} - Y_{8f}\right)\right) K_{wfL} \end{aligned} \qquad \text{(EQ 6-60)}$$

$$\begin{aligned} F_{tR} &= F_{ts} - \delta_{wfR} K_{wfR} \\ &= F_{ts} - \sin\phi\left(X_{1f} - \tan\phi\left(Y_{6f} - Y_{8f}\right)\right) K_{wfR} \end{aligned} \qquad \text{(EQ 6-61)}$$

where "F_{ts}" is the *static* tire reaction force for one side, "δ_{wfL}" & "δ_{wfR}" are the left and right front wheel deflections, and "K_{wfL}" & "K_{wfR}" are the *instantaneous* left and right front wheel rates. Through substitution, the roll resistance couple for the front suspension then becomes (EQ 6-62):

$$RRC_f = 2\sin\phi X_{1f}^{\,2} K_{wf} \qquad \text{(EQ 6-62)}$$

where the front wheel rate in roll is defined (using the average of the left & right motion ratios) by (EQ 6-63) :

$$K_{wf} = K_{sf}\, MR_{sf}^{\,2} + K_{rbf}\, MR_{rbf}^{\,2} \qquad \text{(EQ 6-63)}$$

In (EQ 6-63) the wheel rate is defined as a function of square of the motion ratio, because the spring and wheel rates must be converted to forces using their respective deflections before their moments can be balanced. This can be easily understood by performing a moment balance on a balance beam or "see-saw" which has an asymmetrical pivot point; using rates and deflections instead of forces.

The front roll resistance couple is then defined by (EQ 6-64) as a function of the spring and anti-roll bar rates "K_{sf}" & "K_{rbf}" and their respective (left & right average) motion rations "MR_{sf}" & "MR_{rbf}", where the springs and anti-roll bars act in parallel:

$$RRC_f = 2\sin\phi X_{1f}^{\,2}\left(K_{sf}\, MR_{sf}^{\,2} + K_{rbf}\, MR_{rbf}^{\,2}\right) \qquad \text{(EQ 6-64)}$$

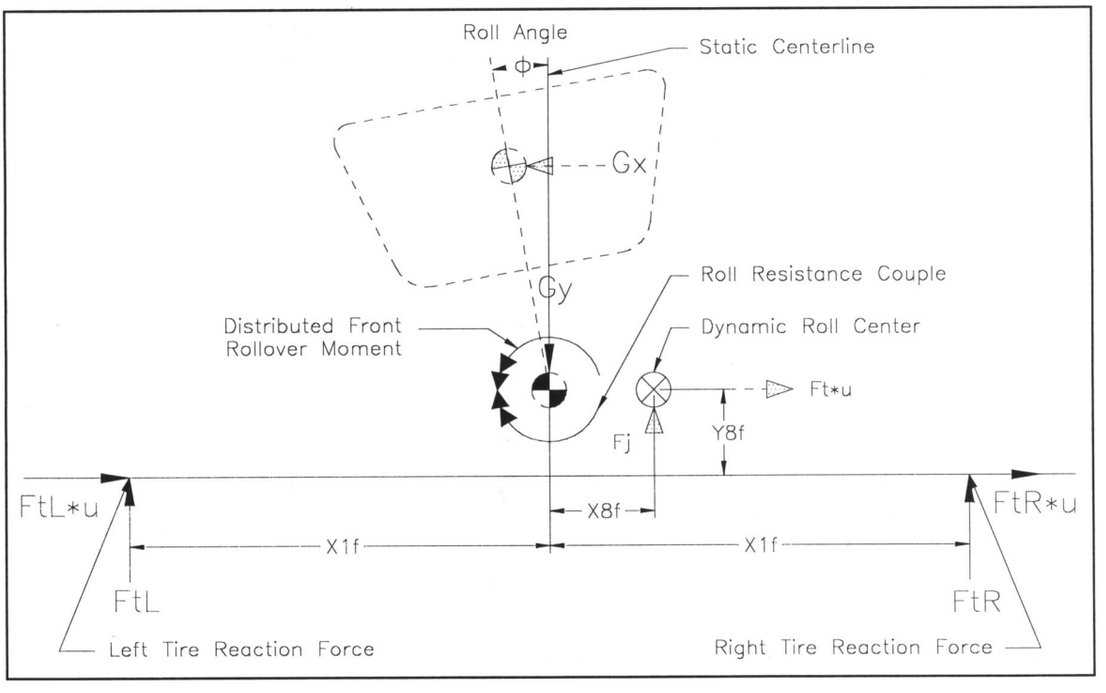

FIGURE 6-5

ROLL RESISTANCE COUPLE

Equation 6-64 is exact at any roll angle. At small angles, we can simplify this equation by assuming that $\sin\phi_{rad} \approx \phi_{rad}$ where "ϕ_{rad}" is a small roll angle in radians. This simplification essentially linearizes the roll resistance couple by removing the "sin" dependency, therefore producing a constant value for all angles. This assumption is only reasonably accurate for small roll angles. For small roll angles then, the simplified version of (EQ 6-64) can be converted from "*lbin/rad*" to "*lbin*/deg" by multiplying by "$\pi/180$". The front roll resistance per degree can now be closely approximated (**for small roll angles only**) using (EQ 6-65):

$$\frac{RR}{\deg_f} = \frac{2\pi X_{1f}{}^2\left(K_{sf} MR_{sf}{}^2 + K_{rbf} MR_{rbf}{}^2\right)}{180} = \frac{lbin}{\deg} \qquad \text{(EQ 6-65)}$$

The resulting vehicle roll angle when laterally accelerated is then defined by (EQ 6-66) (CW=+):

$$\phi = -\left(\frac{M_s\left(G_x(Y_{c.g.} - Y_{8m}) + G_y \tan\phi(Y_{c.g.} - Y_{8m})\right) + F_j X_8}{RR_f/\deg + RR_r/\deg}\right) = \deg$$

(EQ 6-66)

6.23 Longitudinal Load Transfer - Load is transferred longitudinally during braking & acceleration and in bump & droop. Pitching moments about the ground plane are created when the sprung and unsprung masses are longitudinally accelerated (seen in Figure 6-6). Pitching moments are also created about the middle of the wheelbase at ground level, when the sprung mass of a vehicle with a forward or rearward weight bias is vertically accelerated.

The pitching moment equation (taken about the c.g. at ground level) is defined as (EQ 6-67) (CW=+):

$$\sum M = 0 = F_{lf} A - F_{lr} B + G_z\left(M_s Y_{c.g.} + M_{uf} Y_{uf} + M_{ur} Y_{ur}\right) - \left(G_y - 1g\right)\left(M_{uf} A - M_{ur} B\right)$$

(EQ 6-67)

In EQ 6-67, "F_{lf}" & "F_{lr}" are defined as the additional front and rear tire reaction forces due to load transfer, "G_z" & "G_y" are the longitudinal and vertical accelerations in "G's", "$1g$" is the acceleration due to gravity in "G's", "M_{uf}" &"M_{ur}" are the front and rear unsprung masses, and "Y_{uf}" & "Y_{ur}" are the front and rear unsprung mass c.g. heights.

The front and rear tire reaction forces are then solved simultaneously by summing vertical forces equal to zero: $F_{lf} + F_{lr} = \left(G_y - 1g\right)\left(M_s + M_{uf} + M_{ur}\right)$. The front and rear tire forces are defined by (EQ 6-68) and (EQ 6-69):

$$F_{lf} = -\frac{M_s\left(G_z Y_{c.g.} - \left(G_y - 1g\right)B\right) + M_{uf}\left(G_z Y_{uf} - \left(G_y - 1g\right)(A+B)\right) + M_{ur} G_z Y_{ur}}{A+B}$$

(EQ 6-68)

$$F_{lr} = \frac{M_s\left(G_z Y_{c.g.} + \left(G_y - 1g\right)A\right) + M_{ur}\left(G_z Y_{ur} + \left(G_y - 1g\right)(A+B)\right) + M_{uf} G_z Y_{uf}}{A+B}$$

(EQ 6-69)

The longitudinal load transfer from the front to the rear is calculated by (EQ 6-70):

$$LT_z = \frac{F_{lr} - F_{lf}}{2} = \frac{M_s\left(G_z Y_{c.g.} + \left(G_y - 1g\right)/2\,(A-B)\right) + M_{uf}\left(G_z Y_{uf} - \left(G_y - 1g\right)/2\,(A+B)\right)}{A+B} + \frac{M_{ur}\left(G_z Y_{ur} + \left(G_y - 1g\right)/2\,(A+B)\right)}{A+B}$$

(EQ 6-70)

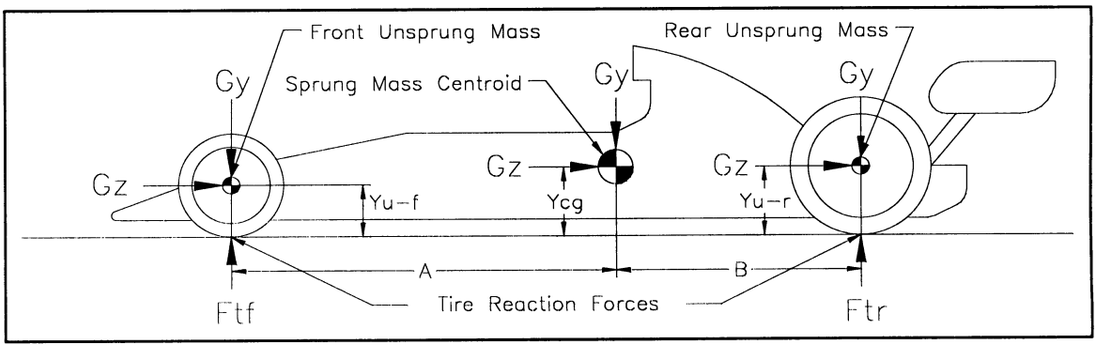

FIGURE 6-6

LONGITUDINAL LOAD TRANSFER DIAGRAM

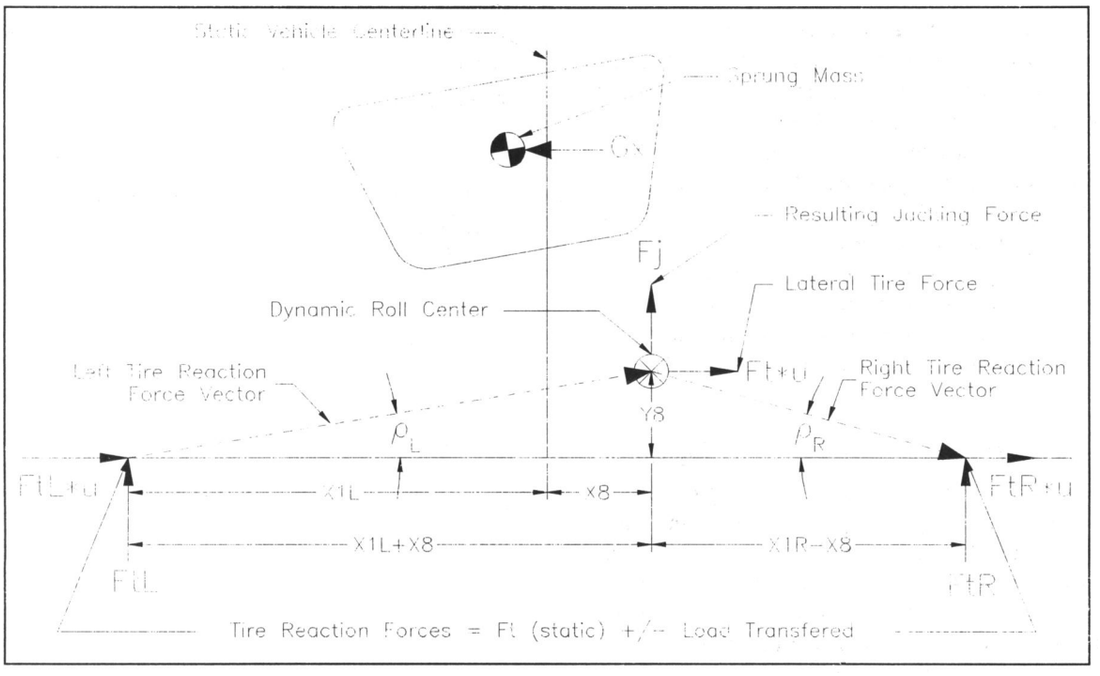

FIGURE 6-7

JACKING FORCE DIAGRAM

6.24 Jacking Forces - Jacking force is the vertical component of the force vector formed between the tire contact patch and the roll center. As a vehicle is laterally accelerated, the front & rear tires generate reaction force vectors which act on the vehicle at their respective roll centers. If the roll center is above ground, the laden tire will produce an upward force vector which is greater in magnitude than the downward force vector produced by the unladen tire (as seen in Figure 6-7). The resulting upward vertical component of these reaction forces raises the respective sprung mass, and produces an additional rollover moment when acting on a laterally displaced roll center. Since these forces are transmitted to the vehicle through the suspension links, they are internally resolved, and do not change the tire loading.

The left and right incident angles between the ground and the tire reaction force vectors "ρ_L" & "ρ_R" are defined by (EQ 6-71 & 6-72):

$$\tan\rho_L = \frac{Y_{8f}}{X_{1Lf} + X_{8f}} = \frac{F_{jL}}{F_{tLf}\mu_f} \qquad \text{(EQ 6-71)}$$

$$\tan\rho_R = \frac{Y_{8f}}{X_{1Rf} - X_{8f}} = \frac{F_{jR}}{-F_{tRf}\mu_f} \qquad \text{(EQ 6-72)}$$

Equations 6-71 & 6-72 can be rewritten to develop a formula for the left and right vertical components of these tire force vectors "F_{jL}" & "F_{jR}" as follows (front shown):

$$F_{jL} = \frac{F_{tLf}\mu_f Y_{8f}}{X_{1Lf} + X_{8f}} \qquad \text{(EQ 6-73)}$$

$$F_{jR} = \frac{-F_{tRf}\mu_f Y_{8f}}{X_{1Rf} - X_{8f}} \qquad \text{(EQ 6-74)}$$

The resulting jacking force can now be found as the sum of these vertical components using (EQ 6-75):

$$F_{jf} = \frac{Y_{8f}\mu_f \left| F_{tLf}\left(X_{1Lf} - X_{8f}\right) - F_{tRf}\left(X_{1Rf} + X_{8f}\right) \right|}{X_{1f}^{\,2} - X_{8f}^{\,2}} \qquad \text{(EQ 6-75)}$$

VII SPRINGS & ANTI-ROLL BARS

The springs and anti-roll bars act on the vehicle through the tire contact patches to generate a roll resistance couple. The spring constants of each need to be calculated to determine the roll resistance of the pair.

7.10 SPRING RATES - The spring constant K_s of a helically wound spring is calculated using (EQ 7-1):

$$K = \frac{d^4 G}{8ND^3} \qquad \text{(EQ 7-1)}$$

where "N" is the number of active spring coils, "d" is the diameter of the spring wire, "D" is the center to center diameter of the spring, and "G" is the modulus of rigidity of the spring material.

7.20 ANTI-ROLL BAR RATES - An anti-roll bar is a combination of two springs acting in series. The first spring is the torque tube which produces resistance per degree of rotation. The second spring is the blade which transmits the linear motion of the suspension to the torsional rotation of the torque tube. Anti-roll bars are typically adjustable in race cars to fine tune the balance of the vehicle during a race. One method of achieving this adjustability (as seen in Figure 7-1) is accomplished by rotating one of the tapered blades about its longitudinal axis at its attachment point to the torque tube. This reduces or increases its spring constant by effectively changing the blades moment of inertia with respect to the load at the tip of the blade.

The spring constant K_{bl} of the tapered blade in its stiffest vertical position is calculated by solving for the tip deflection caused by a unit load using Castigliano's Theorem. Per Castigliano's Theorem, the deflection in this elastic tapered beam, can be found by obtaining the partial derivative of the total strain energy with respect to the load at the end of the beam. Because this particular beam is tapered, the sum of the strain energies due to shear and bending must be integrated along the length of the tapered blade. The deflection at the tip of the blade "δ_{bl}" for a unit load "P" is found using (EQ 7-2):

$$\delta_{bl}=\frac{\partial U_s}{\partial P}+\frac{\partial U_m}{\partial P}=\int_0^l \frac{kV}{GA}\frac{\partial V}{\partial P}\partial x+\int_0^l \frac{M}{EI}\frac{\partial M}{\partial P}\partial x \qquad \text{(EQ 7-2)}$$

In this equation, "k" is the correction coefficient for strain energy due to shear and equals 1.5 for a beam of rectangular cross section. "V" is the shear force, "G" is the modulus of rigidity, "A" is the cross sectional area of the blade (equal to "bH"), "l" is the length of the blade, "M" is the bending moment, "E" is the modulus of elasticity, and "I" is the moment of inertia as some point "x" from the blade tip.

The moment of inertia at a point "x" from the blade tip along its length is defined by (EQ 7-3):

$$I=bH^3/12=b\left(x\left(H_r-H_t\right)/l+H_t\right)^3/12 \qquad \text{(EQ 7-3)}$$

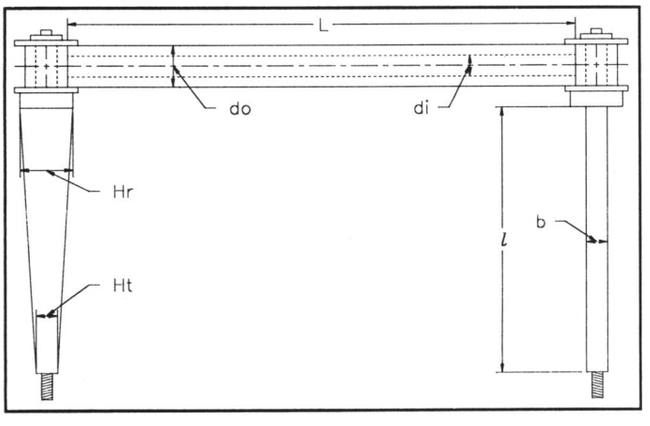

FIGURE 7-1

ADJUSTABLE ANTI-ROLL BAR

where "b" is the thickness of the blade, "l" is the length of the blade, "H_r" is the blade height at the root, and "H_t" is the height of the blade at the tip.

The deflection at the tip of the blade "δ_{bl}" due to the load "P"can now be found by substituting (EQ 7-3) into (EQ 7-2) and integrating along the length of the blade. This equation is found to be (EQ 7-4):

$$\delta_{bl}=\frac{kPl}{Gb\left(H_r-H_t\right)}\ln\left(\frac{H_r}{H_t}\right)+\frac{12Pl^3}{Eb\left(H_r-H_t\right)^3}\left(\ln\left(\frac{H_r}{H_t}\right)+\frac{2H_t}{H_r}-\frac{H_t^2}{2H_r^2}-\frac{3}{2}\right)$$

(EQ 7-4)

The resulting spring rate of the tapered blade can now be calculated using (EQ 7-5):

$$K_{bl}=\frac{P}{\delta_{bl}}=\frac{1}{\frac{kl}{Gb\left(H_r-H_t\right)}\ln\left(\frac{H_r}{H_t}\right)+\frac{12l^3}{Eb\left(H_r-H_t\right)^3}\left(\ln\left(\frac{H_r}{H_t}\right)+\frac{2H_t}{H_r}-\frac{H_t^2}{2H_r^2}-\frac{3}{2}\right)}$$

(EQ 7-5)

The linear spring constant of the torque tube K_{tt} is found to be (EQ 7-6)

$$K_{tt}=\frac{GI}{l^2L/2}=\frac{2GI}{l^2L} \qquad \text{(EQ 7-6)}$$

For a tube in torsion, the linear spring constant of the torque tube is found to be (EQ 7-7):

$$K_{tt}=\frac{\pi G\left(d_o^{\,4}-d_i^{\,4}\right)}{32l^2L} \qquad \text{(EQ 7-7)}$$

where "G" is the torsional modulus, "d_o" and "d_i" are the outer and inner tube diameters, "l" is the length of the blade and "L" is the *true* length of the torque tube.

For an anti-roll bar, the effective length of the torque tube equals 1/2 of the true length, because only 1/2 of the tube resists each wheel motion. This is due to the fact that (if the tube bearings are assumed to be frictionless) each end of the torque tube resists an equal but opposite moment and forms a couple. This couple is formed after the left and right moments have equalized. This equilibrium is achieved once the center of the torque tube has rotated by an amount equivalent to the difference between the left and right wheel displacements. This symmetry is equivalent to fixing the center of tube and using 1/2 of the torque tube to resist each wheel motion.

The resulting spring constant for the anti-roll bar assembly K_{rb} is then found to be (EQ 7-8):

$$K_{rb}=\frac{K_{tt}K_{bl}}{K_{tt}+K_{bl}} \qquad \text{(EQ 7-8)}$$

7.30 MOTION RATIOS - Motion ratio is an important part of any discussion of vehicle dynamics, because this ratio determines the effective wheel rates for a given spring rate. Motion ratio has classically been defined as the displacement of the spring divided by the displacement of the respective wheel, and is usually represented as a constant fraction. While this classic definition is often quoted, it is actually not particularly accurate and can be very misleading.

As a ratio of the spring displacement over the wheel displacement, this classic definition actually represents the average of the instantaneous motion ratios over the displacement range measured. For example, if a spring is displaced .75 inches from its static length for a drop in the chassis of 1.0 inch, the average of the instantaneous motion ratios between the static ride height and the ride height which has been displaced downward 1.0 inch would be 0.75.

It becomes clear, when looked at as a function of these gross displacements, that this classic definition cannot generate the instantaneous motion ratio at 1 inch of chassis deflection, because the resulting answer by definition depends on some starting point over which to measure the wheel and spring displacements.

This classic definition actually produces a number which represents the instantaneous wheel rate at some point between the starting and final displacements. *Assuming* that the change in motion ratio stays linear over this range, this classic definition will in fact give the instantaneous motion ratio at the *middle* of this range. However, since motion ratios are rarely linear, this method is not acceptably accurate.

For accurate modeling of vehicle dynamics then, a definition of motion ratio is required which represents the true motion ratio of a suspension at any instant of time regardless of the suspension's geometric linearity.

The equation for the instantaneous motion ratio can be developed by balancing the forces present in the suspension components & spring against the forces present at the tire contact patch. Since the forces acting on the tire & spring are directly proportional to their displacements, an equation can be written for the instantaneous motion ratio using a tire force of unity by balancing these forces & moments. This method will be used to calculate the instantaneous motion ratios for the outboard spring/damper, push-rod, pull-rod, and rocker arm types of suspensions.

7.31 <u>Outboard Spring/Damper Motion Ratio</u> - Figure 7-2 describes the nomenclature which will be used to calculate the instantaneous motion ratio for an outboard spring/damper type suspension.

The vertical unity force at the tire contact patch must first be resolved into the horizontal & vertical components acting on the kingpin ball joints. This force will be resolved by taking moments about the lower kingpin ball joint because the upper control arm is the only two force member connected to the kingpin. This moment balance is given by (EQ 7-9) (CW=+):

$$F_t\left(X_1-|X_4|\right)=F_{up}\sqrt{\left(X_4-X_5\right)^2+\left(Y_5-Y_4\right)^2} \qquad \text{(EQ 7-9)}$$

where "F_t" is the force at the center of the tire contact patch, & "F_{up}" is the force at the upper ball joint perpendicular to the moment arm formed between the upper and lower ball joints.

Note: This force is not necessarily the same as the one at the upper ball joint which acts along the upper control arm axis "F_u", because the angle between the upper control arm and the line which connects the upper and lower ball joints is not always perpendicular.

The resulting perpendicular force found in (EQ 7-9) must therefore be resolved into the force at the upper ball joint which acts parallel to the control arm "F_u" using (EQ 7-10) (CW=+):

$$F_t\left(X_1-|X_4|\right)=F_u\cos\left(SAI'-\beta-\left(\theta-\theta'\right)\right)\sqrt{\left(X_4-X_5\right)^2+\left(Y_5-Y_4\right)^2} \qquad \text{(EQ 7-10)}$$

where "SAI'" is the static steering axis inclination, "θ" & "θ'" are the instantaneous & static camber angles. The angle which the upper control arm makes with horizontal "β", is defined by (EQ 7-11 & 7-12):

$$\beta_L=\arctan\left(\frac{Y_{5L}-Y_{3L}}{-\left(X_{5L}-X_{3L}\right)}\right) \qquad \text{(EQ 7-11)}$$

$$\beta_R=\arctan\left(\frac{Y_{5R}-Y_{3R}}{X_{5R}-X_{3R}}\right) \qquad \text{(EQ 7-12)}$$

The forces at the lower kingpin ball joint can now be found by summing the horizontal & vertical components of the forces present at the upper & lower ball joints using (EQ 7-13 & 7-14):

$$F_{lx}=F_{ux}=F_u\cos\beta \qquad \text{(EQ 7-13)}$$

$$F_{ly}=F_l+F_{uy}=F_l+F_u\sin\beta \qquad \text{(EQ 7-14)}$$

The vertical & horizontal forces at the lower kingpin ball joint can now be balanced against the resistive spring forces by taking moments about the lower control arm inner pickup point using (EQ 7-15) (CW=+):

$$F_{ly}\left|X_4-X_2\right|-F_{lx}\left(Y_4-Y_2\right)=F_s\left(ArmS\right) \qquad \text{(EQ 7-15)}$$

Note: the directions of "F_{lx}" & "F_{ly}" displayed in Figure 7-2 are correct for studying the hub carrier free body diagram, but must be reversed when analyzing the forces acting on the lower control arm at the lower kingpin ball joint.

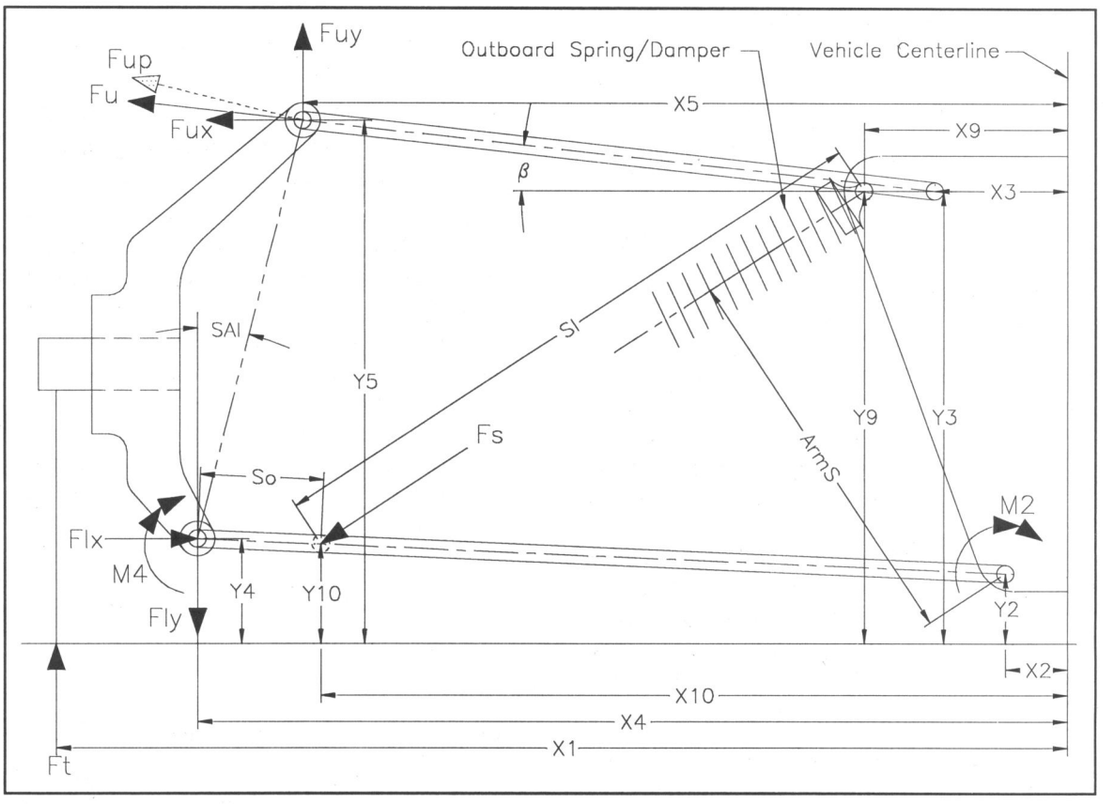

FIGURE 7-2

OUTBOARD SPRING MOTION RATIO CALCULATION PARAMETERS

where "F_s" is the spring force acting along the spring/damper axis. "*ArmS*" is the moment arm through which the spring produces its resisting torque about the lower control arm inner pick up point. "*ArmS*" is defined as the distance from the lower control arm inner pick up point to the line of action of the spring axis. This moment arm is found through the law of cosines to be (EQ 7-16):

$$ArmS = (L_l - S_o)\sin\left(\arccos\left(\frac{(L_l - S_o)^2 + S_l^2 - (Y_9 - Y_2)^2 - (X_9 - X_2)^2}{2(L_l - S_o)S_l}\right)\right)$$

(EQ 7-16)

where "L_l" is the lower control arm length, "S_o" is the offset of the lower spring mount from the end of the control arm, & "S_l" is the instantaneous length of the spring.

By substituting (EQ 7-13) & (EQ 7-14) into (EQ 7-15) the spring force is found to be (EQ 7-17):

$$F_s = \frac{(F_l + F_u \sin\beta)|X_4 - X_2| - F_u \cos\beta(Y_4 - Y_2)}{ArmS} = \frac{(F_l)|X_4 - X_2| + F_u(\sin\beta|X_4 - X_2| - \cos\beta(Y_4 - Y_2))}{ArmS}$$

(EQ 7-17)

The spring force can now be defined as a function of the tire force by substituting (EQ 7-10) into (EQ 7-17) to yield (EQ 7-18):

$$F_s = \frac{(F_l)\left(|X_4 - X_2| + \frac{(X_1 - |X_4|)(\sin\beta|X_4 - X_2| - \cos\beta(Y_4 - Y_2))}{\cos(SA\,I' - \beta - (\theta - \theta'))\sqrt{(X_4 - X_5)^2 + (Y_5 - Y_4)^2}}\right)}{ArmS}$$

(EQ 7-18)

The instantaneous motion ratio for an outboard spring/damper suspension is defined as a ratio of the tire & spring forces to be (EQ 7-19) (left shown, right is similar):

$$MR_{L(outboard-spring)} = \frac{F_{tL}}{F_{sL}} = \frac{(L_l - S_o)\sin\left(\arccos\left(\frac{(L_l - S_o)^2 + S_{lL}^2 - (Y_{9L} - Y_{2L})^2 - (X_{9L} - X_{2L})^2}{2(L_l - S_o)S_{lL}}\right)\right)}{|X_{4L} - X_{2L}| + \left(\frac{(X_1 - |X_{4L}|)(\sin\beta_L|X_{4L} - X_{2L}| - \cos\beta_L(Y_{4L} - Y_{2L}))}{\cos(SA\,I' - \beta_L - (\theta_L - \theta'))\sqrt{(X_{4L} - X_{5L})^2 + (Y_{5L} - Y_{4L})^2}}\right)}$$

(EQ 7-19)

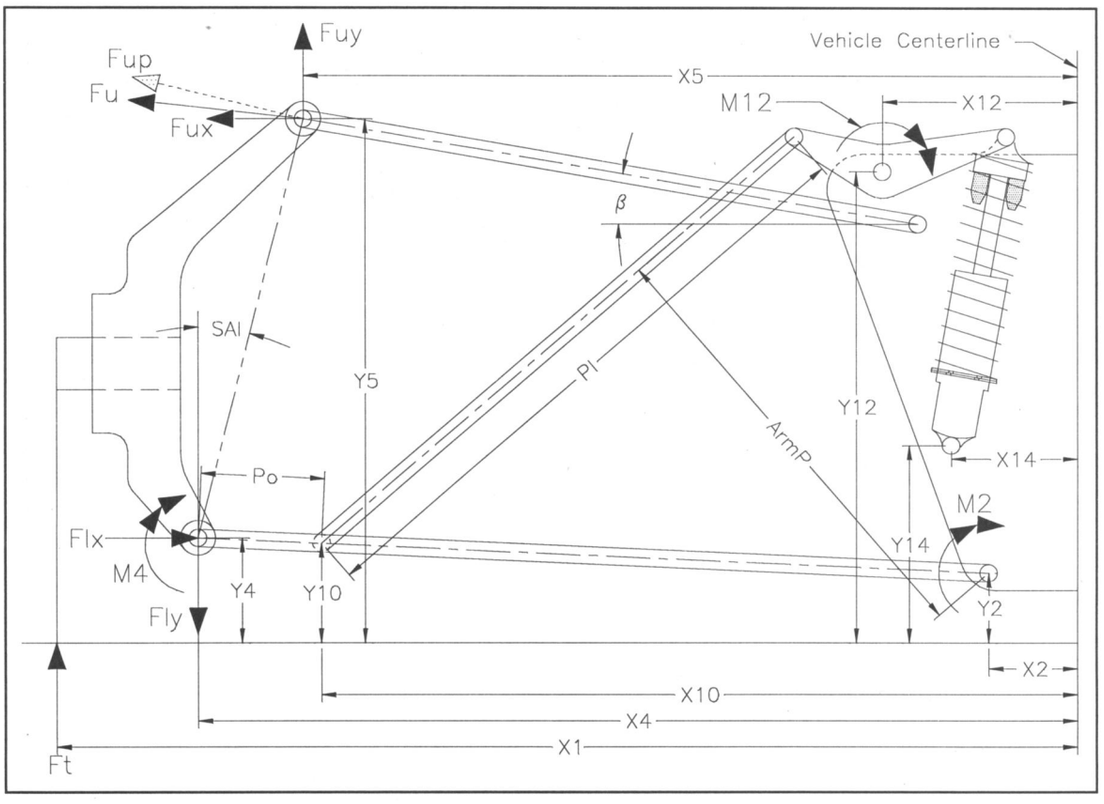

FIGURE 7-3

PUSH-ROD MOTION RATIO CALCULATION PARAMETERS

7.32 Push-Rod Suspension Motion Ratio - Figures 7-3 & 7-4 describe the nomenclature which will be used to calculate the instantaneous motion ratio for push-rod type suspensions.

The same equations used to determine the forces at the lower kingpin pickup point in the outboard spring suspension are used to determine these forces for a push-rod suspension. Therefore, equations 7-9 through 7-14 will not be repeated.

The forces present at the lower kingpin ball joint are balanced against the force in the push-rod by taking moments about the lower inner pickup point using (EQ 7-20) (CW=+):

$$F_{ly}\left|X_4 - X_2\right| - F_{lx}\left(Y_4 - Y_2\right) = F_p\left(ArmP\right) \qquad \text{(EQ 7-20)}$$

where "F_p" is the push-rod force acting along its axis. "$ArmP$" is the moment arm through which the push-rod produces its resisting torque about the lower control arm inner pickup point. This moment arm is found through the law of cosines to be (EQ 7-21):

$$ArmP = \left(L_l - P_o\right)\sin\left(\arccos\left(\frac{\left(L_l - P_o\right)^2 + P_l^2 - \left(Y_9 - Y_2\right)^2 - \left(X_9 - X_2\right)^2}{2\left(L_l - P_o\right)P_l}\right)\right) \qquad \text{(EQ 7-21)}$$

where "P_o" is the offset of the lower push-rod mount from the end of the control arm. "P_l" is the push-rod length & "$X_9 \& Y_9$" is the location of the upper push-rod connection to the bell crank.

The location of the upper push-rod connection follows similar naming conventions used for the outboard spring pickup, however its location is determined by the rotation of the bell-crank, as defined by (EQ 7-22 & 23):

$$X_{9L} = X_{12L} - R_p\cos\lambda_L \qquad \text{(EQ 7-22)}$$

$$X_{9R} = X_{12R} + R_p\cos\lambda_R \qquad \text{(EQ 7-22A)}$$

$$Y_{9L} = Y_{12L} + R_p\sin\lambda_L \qquad \text{(EQ 7-23)}$$

In the previous equations, "R_p" is the crank arm length on the push-rod side of the bell crank and "λ" is the angular position of the push-rod crank relative to horizontal.

The push-rod force can now be found by substituting (EQ 7-13) & (EQ 7-14) into (EQ 7-20) to produce (EQ 7-24):

$$F_p = \frac{\left(F_l + F_u\sin\beta\right)\left|X_4 - X_2\right| - F_u\cos\beta\left(Y_4 - Y_2\right)}{ArmP} = \frac{\left(F_l\right)\left|X_4 - X_2\right| + F_u\left(\sin\beta\left|X_4 - X_2\right| - \cos\beta\left(Y_4 - Y_2\right)\right)}{ArmP} \qquad \text{(EQ 7-24)}$$

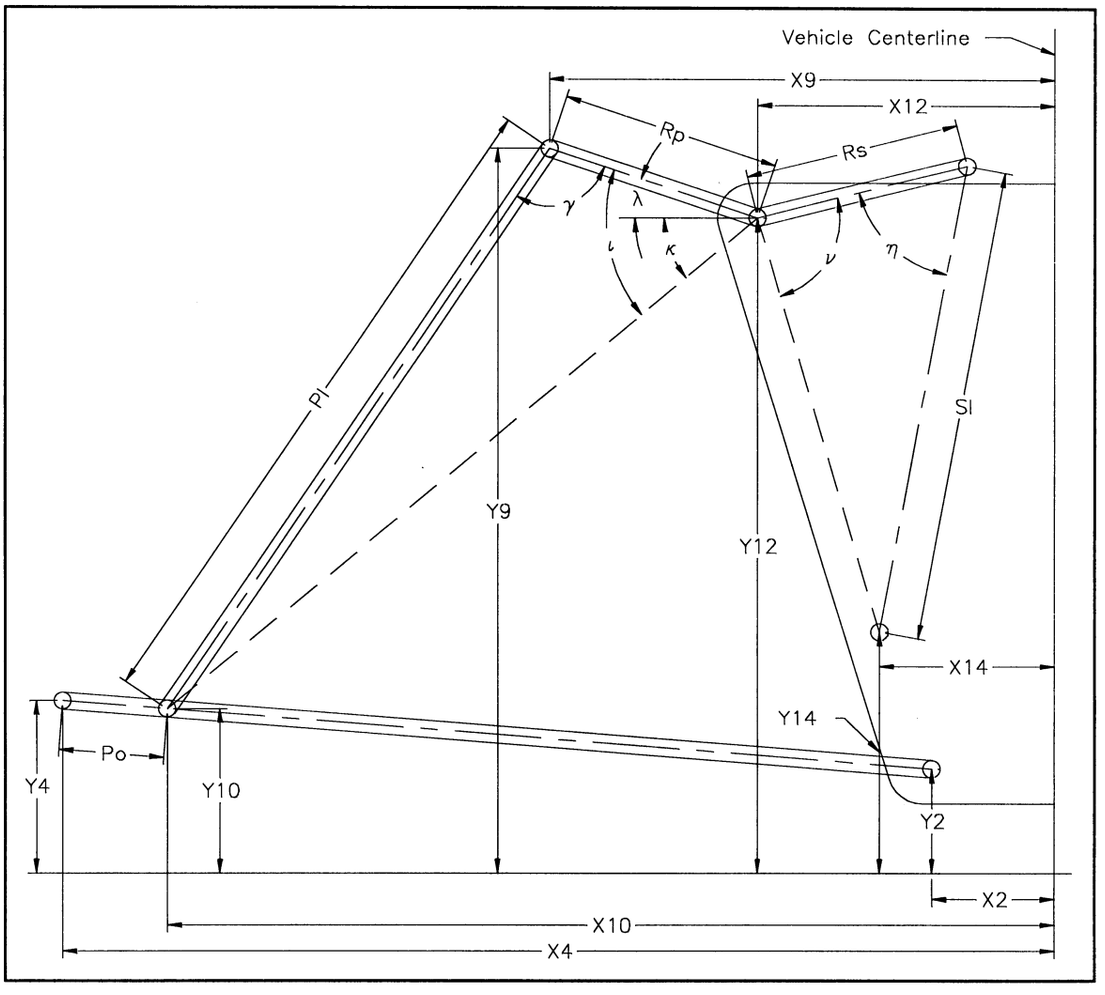

FIGURE 7-4

PUSH-ROD BELL CRANK DIAGRAM

The push-rod force can now be found as a function of the tire force "F_t"by substituting (EQ 7-10) into (EQ 7-24) to produce (EQ 7-25):

$$F_p = \frac{(F_t)\left(|X_4 - X_2| + \dfrac{(X_1 - |X_4|)(\sin\beta|X_4 - X_2| - \cos\beta(Y_4 - Y_2))}{\cos(SAI' - \beta - (\theta - \theta'))\sqrt{(X_4 - X_5)^2 + (Y_5 - Y_4)^2}}\right)}{ArmP}$$

(EQ 7-25)

We must now develop a relationship which balances the push-rod forces, against the resisting forces in the spring by taking moments about the bell crank pivot point. To do this, the push-rod/bell crank and spring/bell crank incident angles must be calculated along with the relative angles of each crank and the spring length. These angles are shown in Figure 7-4.

The push-rod/crank incident angle "γ" is found through the law of cosines using (EQ 7-26):

$$\gamma = \arccos\left(\frac{P_l^2 + R_p^2 - (X_{10} - X_{12})^2 - (Y_{12} - Y_{10})^2}{2P_lR_p}\right) \quad \text{(EQ 7-26)}$$

where "P_l" and "R_p" are the push-rod length and crank arm length on the push-rod side of the bell crank.

The angular position of the push-rod crank relative to horizontal "λ" is defined by (EQ 7-27):

$$\lambda = \iota - \kappa$$
$$= \arccos\left(\frac{R_p^2 + (X_{10} - X_{12})^2 + (Y_{12} - Y_{10})^2 - P_l^2}{2R_p\sqrt{(X_{10} - X_{12})^2 + (Y_{12} - Y_{10})^2}}\right) - \arctan\left(\frac{Y_{12} - Y_{10}}{|X_{10} - X_{12}|}\right)$$

(EQ 7-27)

In EQ 7-27, "ι" is the incident angle between the push-rod crank and the imaginary line connecting the crank pivot point with the lower push-rod pickup point , and "κ" is the angle which this imaginary line makes with horizontal.

The spring/crank incident angle "η" is found through the law of cosines to be (EQ 7-28):

$$\eta = \arccos\left(\frac{S_l^2 + R_s^2 - (X_{12} - X_{14})^2 - (Y_{12} - Y_{14})^2}{2 S_l R_s}\right) \qquad \text{(EQ 7-28)}$$

where "S_l" and "R_s" are the spring length and crank arm length on the spring side of the bell crank.

The angular position of the spring crank relative to the imaginary line connecting the crank pivot point with the lower spring mount "ν" is defined as a function of the bell-crank rotation by (EQ 7-29):

$$\nu = \nu' - (\lambda - \lambda')$$
$$= \arccos\left(\frac{R_s^2 + (X'_{12} - X'_{14})^2 + (Y'_{12} - Y'_{14})^2 - (S'_l)^2}{2 R_s \sqrt{(X'_{12} - X'_{14})^2 + (Y'_{12} - Y'_{14})^2}}\right) - (\lambda - \lambda') \qquad \text{(EQ 7-29)}$$

where "ν'" is the static relative angular position of the spring crank, and $(\lambda - \lambda')$ is the bell crank rotation (as measured from the static push-rod crank angle "λ'").

The spring length "S_l"can now be found through the law of cosines by (EQ 7-30):

$$S_l = \sqrt{R_s^2 + (X_{12} - X_{14})^2 + (Y_{12} - Y_{14})^2 - 2 R_s \cos\nu \sqrt{(X_{12} - X_{14})^2 + (Y_{12} - Y_{14})^2}} \qquad \text{(EQ 7-30)}$$

The spring force "F_s" can now be defined as a function of the push-rod force "F_p" by taking moments about the bell crank pivot point (EQ 7-31):

$$F_p R_p(\sin\gamma) = F_s R_s(\sin\eta) \qquad \text{(EQ 7-31)}$$

The spring force can then be defined with respect to the tire force by substituting (EQ 7-25) into (EQ 7-31) to yield (EQ 7-32):

$$F_s = \frac{R_p(\sin\gamma)}{R_s(\sin\eta)}[F_p]$$
$$= \frac{R_p(\sin\gamma)\left[(F_l)\left(|X_4 - X_2| + \frac{(X_1 - |X_4|)(\sin\beta|X_4 - X_2| - \cos\beta(Y_4 - Y_2))}{\cos(SA I' - \beta - (\theta - \theta'))\sqrt{(X_4 - X_5)^2 + (Y_5 - Y_4)^2}}\right)\right]}{R_s(\sin\eta)\left[(L_l - P_o)\sin\left(\arccos\left(\frac{(L_l - P_o)^2 + P_l^2 - (Y_9 - Y_2)^2 - (X_9 - X_2)^2}{2(L_l - P_o)P_l}\right)\right)\right]} \qquad \text{(EQ 7-32)}$$

The instantaneous motion ratio for push-rod suspensions can now be found as a ratio of the tire and spring forces using (EQ 7-33) (left shown, right is similar):

$$MR_{L(push-rod)} = \frac{F_{tL}}{F_{sL}}$$
$$= \frac{R_s(\sin\eta_L)(L_l - P_o)\sin\left(\arccos\left(\frac{(L_l - P_o)^2 + P_l^2 - (Y_{9L} - Y_{2L})^2 - (X_{9L} - X_{2L})^2}{2(L_l - P_o)P_l}\right)\right)}{R_p(\sin\gamma_L)\left(|X_{4L} - X_{2L}| + \frac{(X_1 - |X_{4L}|)(\sin\beta_L|X_{4L} - X_{2L}| - \cos\beta_L(Y_{4L} - Y_{2L}))}{\cos(SA I' - \beta_L - (\theta_L - \theta'))\sqrt{(X_{4L} - X_{5L})^2 + (Y_{5L} - Y_{4L})^2}}\right)} \qquad \text{(EQ 7-33)}$$

7.33 Pull-Rod Suspension Motion Ratio - Figures 7-5 & 7-6 describe the nomenclature which will be used to calculate the instantaneous motion ratio for pull-rod type suspensions. The method for calculating the pull-rod motion ratio is nearly identical to that used for push-rod suspensions except that the tire forces are transferred to the springs through the upper control arm rather than through the lower control arm.

Because the lower control arm is the only two force member attached to the kingpin in a pull-rod suspension, the vertical unity force at the tire will be resolved into the horizontal & vertical components acting on the lower kingpin ball joint by taking moments about the upper kingpin ball joint. This moment balance is given by (EQ 7-34) (CW=+):

$$F_t(X_1 - |X_5|) = F_{lp}\sqrt{(X_4 - X_5)^2 + (Y_5 - Y_4)^2} \qquad \text{(EQ 7-34)}$$

where "F_t" is the force at the center of the tire contact patch, & "F_{lp}" is the force at the lower ball joint perpendicular to the moment arm between the upper and lower ball joints.

The resulting perpendicular force found in (EQ 7-34) must be resolved into the force at the lower ball joint which acts parallel to the control arm "F_l" using (EQ 7-35) (CW=+):

$$F_t(X_1 - |X_5|) = F_l \cos(\alpha - SA I' + (\theta - \theta'))\sqrt{(X_4 - X_5)^2 + (Y_5 - Y_4)^2} \qquad \text{(EQ 7-35)}$$

The angle which the lower control arm makes with horizontal "α" is defined by (EQ 7-36 & 7-37):

$$\alpha_L = \arctan\left(\frac{Y_{4L} - Y_{2L}}{-(X_{4L} - X_{2L})}\right) \qquad \text{(EQ 7-36)}$$

$$\alpha_R = \arctan\left(\frac{Y_{4R} - Y_{2R}}{X_{4R} - X_{2R}}\right) \qquad \text{(EQ 7-37)}$$

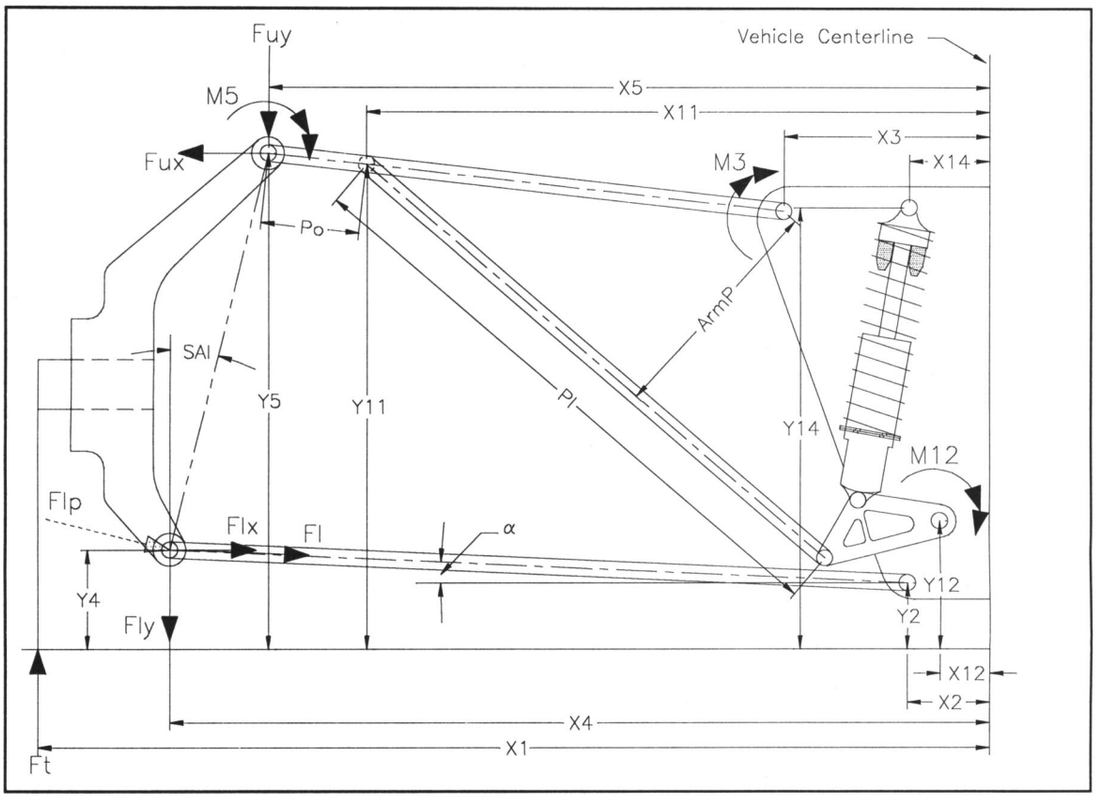

FIGURE 7-5

PULL-ROD MOTION RATIO CALCULATION PARAMETERS

The forces at the upper kingpin ball joint can now be found by summing the horizontal & vertical components of the forces present at the upper & lower ball joints using (EQ 7-38) & (EQ 7-39)

$$F_{ux} = F_{lx} = F_l \cos\alpha \qquad \text{(EQ 7-38)}$$

$$F_{uy} = F_t - F_{ly} = F_t - F_l \sin\alpha \qquad \text{(EQ 7-39)}$$

The forces present at the upper kingpin ball joint can now be balanced against the force in the pull-rod by taking moments about the upper inner pickup point (EQ 7-40) (CW=+):

$$F_{uy}\left|X_5 - X_3\right| + F_{ux}\left(Y_5 - Y_3\right) = F_p(ArmP) \qquad \text{(EQ 7-40)}$$

where "F_p" is the pull-rod force acting along its axis. "$ArmP$" is the moment arm through which the pull-rod produces its resisting torque about the upper control arm inner pickup point. This moment arm is found through the law of cosines to be (EQ 7-41):

$$ArmP = \left(L_u - P_o\right)\sin\left(\arccos\left(\frac{\left(L_u - P_o\right)^2 + P_l^2 - \left(Y_3 - Y_9\right)^2 - \left(X_9 - X_3\right)^2}{2\left(L_u - P_o\right)P_l}\right)\right) \qquad \text{(EQ 7-41)}$$

where "P_o" is the offset of the upper pull-rod mount from the end of the upper control arm. "P_l" is the push-rod length, & "$X_9 \& Y_9$" is the location of the lower pull-rod connection to the bell crank.

The position of the lower end of the pull-rod connection to the bell crank is defined by (EQ 7-42 & 7-43)

$$X_{9L} = X_{12L} - R_p \cos\lambda_L \qquad \text{(EQ 7-42)}$$

$$X_{9R} = X_{12R} + R_p \cos\lambda_R \qquad \text{(EQ 7-42A)}$$

$$Y_{9L} = Y_{12L} - R_p \sin\lambda_L \qquad \text{(EQ 7-43)}$$

In the previous equations, "R_p" is the crank arm length on the pull-rod side of the bell crank and "λ" is the angular position of the pull-rod crank relative to horizontal.

The pull-rod force can now be found by substituting (EQ 7-38) & (EQ 7-39) into (EQ 7-40) to produce (EQ 7-44):

$$F_p = \frac{\left(F_t - F_l \sin\alpha\right)\left|X_5 - X_3\right| + F_l \cos\alpha\left(Y_5 - Y_3\right)}{ArmP} = \frac{\left(F_t\right)\left|X_5 - X_3\right| + F_l\left(\cos\alpha\left(Y_5 - Y_3\right) - \sin\alpha\left|X_5 - X_3\right|\right)}{ArmP} \qquad \text{(EQ 7-44)}$$

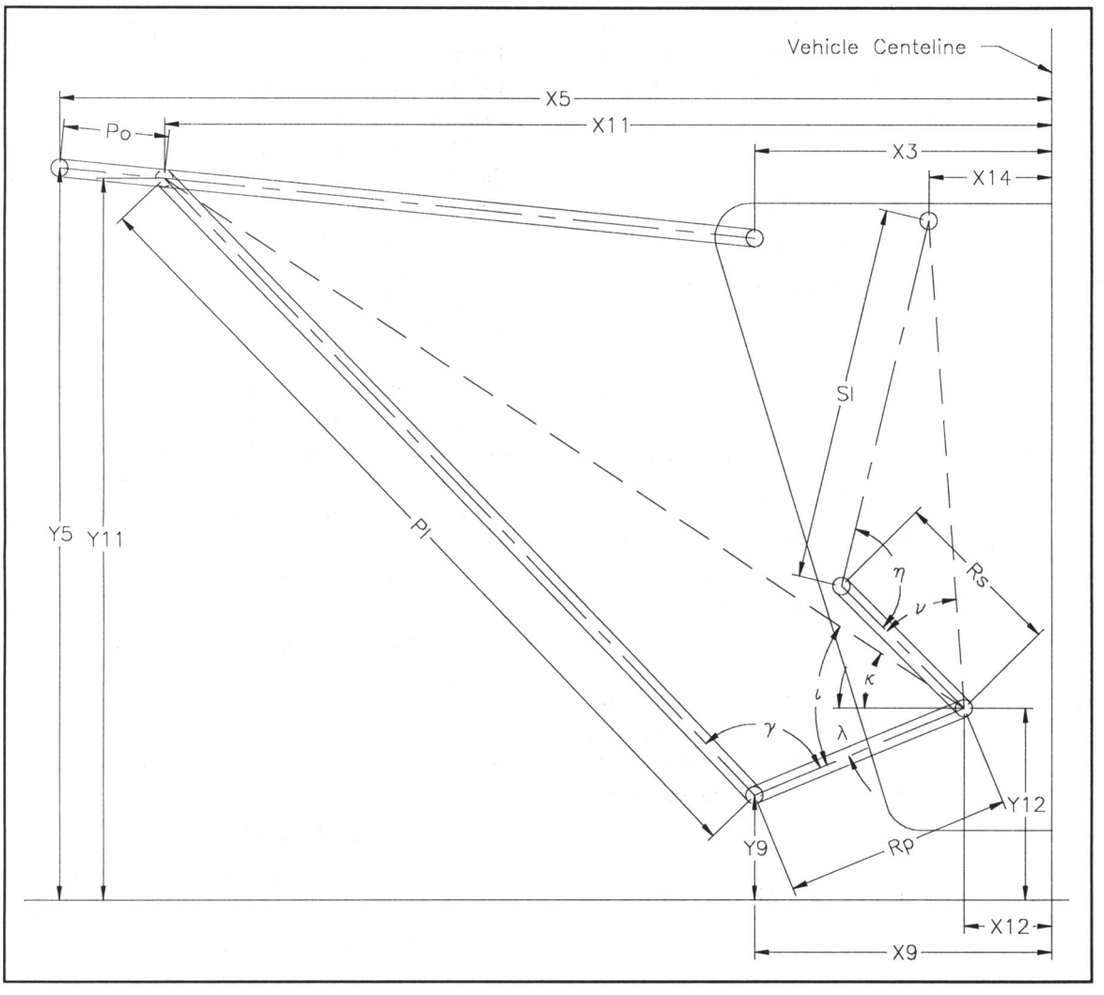

FIGURE 7-6

PULL-ROD BELL CRANK DIAGRAM

The pull-rod force can now be found as a function of the tire force "F_t" by substituting (EQ 7-35) into (EQ 7-44) to produce (EQ 7-45):

$$F_p = \frac{(F_t)\left(|X_5 - X_3| + \dfrac{(X_1 - |X_5|)(\cos\alpha(Y_5 - Y_3) - \sin\alpha|X_5 - X_3|)}{\cos(\alpha - SAI' + (\theta - \theta'))\sqrt{(X_4 - X_5)^2 + (Y_5 - Y_4)^2}}\right)}{ArmP}$$

(EQ 7-45)

We must now develop a relationship between the pull-rod and spring forces, by taking moments about the bell crank pivot point. Once again, the dependent variables must be calculated first. These variables are shown in Figure 7-6.

The pull-rod/crank incident angle "γ" is found through the law of cosines to be (EQ 7-46):

$$\gamma = \arccos\left(\frac{P_l^2 + R_p^2 - (X_{11} - X_{12})^2 - (Y_{11} - Y_{12})^2}{2P_l R_p}\right) \quad \text{(EQ 7-46)}$$

where "P_l" and "R_p" are now the pull-rod and crank arm lengths on the pull-rod side of the bell crank.

The angular position of the pull-rod crank relative to horizontal "λ" is defined by (EQ 7-47):

$$\lambda = \iota - \kappa$$
$$= \arccos\left(\frac{R_p^2 + (X_{11} - X_{12})^2 + (Y_{11} - Y_{12})^2 - P_l^2}{2R_p\sqrt{(X_{11} - X_{12})^2 + (Y_{11} - Y_{12})^2}}\right) - \arctan\left(\frac{Y_{11} - Y_{12}}{|X_{11} - X_{12}|}\right)$$

(EQ 7-47)

In EQ 7-47, "ι" is defined as the incident angle between the pull-rod crank and the imaginary line connecting the crank pivot point with the upper pull-rod pickup point, and "κ" is the angle which this imaginary line makes with horizontal.

The spring/crank incident angle "η" is found with the same equation (EQ 7-28) used in the push-rod method.

The angular position of the spring crank relative to the imaginary line connecting the crank pivot point with the lower spring mount "ν" is defined by (EQ 7-44) as a function of the bell crank rotation to be (EQ 7-48):

$$\nu = \nu' + (\lambda - \lambda')$$
$$= \arccos\left(\frac{R_s^2 + (X'_{12} - X'_{14})^2 + (Y'_{12} - Y'_{14})^2 - (S'_l)^2}{2R_s\sqrt{(X'_{12} - X'_{14})^2 + (Y'_{12} - Y'_{14})^2}} \right) + (\lambda - \lambda')$$

(EQ 7-48)

In this equation, "ν'" is the static relative angular position of the spring crank, and $(\lambda - \lambda')$ is the bell crank rotation (as measured from the static pull-rod crank angle "λ'") **Note:** this angle is no longer the difference between the static angle and the rotation angle used for the push-rod suspension, but the sum of these two.

The spring length can now be found with the same equation (EQ 7-30) used for the push-rod method. The spring force "F_s" is also defined as a function of the push-rod force "F_p" with the same equation (EQ 7-31) used for the push-rod method.

The spring force can then be defined with respect to the tire force by substituting (EQ 7-45) into (EQ 7-31) to yield (EQ 7-49):

$$F_s = \frac{R_p(\sin\gamma)}{R_s(\sin\eta)}[F_p]$$
$$= \frac{R_p(\sin\gamma)\left[(F_l)\left(|X_5 - X_3| + \frac{(X_1 - |X_5|)(\cos\alpha(Y_5 - Y_3) - \sin\alpha|X_5 - X_3|)}{\cos(\alpha - SAI' + (\theta - \theta'))\sqrt{(X_4 - X_5)^2 + (Y_5 - Y_4)^2}} \right) \right]}{R_s(\sin\eta)\left[(L_u - P_o)\sin\left(\arccos\left(\frac{(L_u - P_o)^2 + P_l^2 - (Y_3 - Y_9)^2 - (X_9 - X_3)^2}{2(L_u - P_o)P_l} \right) \right) \right]}$$

(EQ 7-49)

The instantaneous motion ratio for pull-rod suspensions can now be found as a ratio of the tire and spring forces to be (EQ 7-50) (left shown, right is similar):

$$MR_{L(pull-rod)} = \frac{F_{tL}}{F_{sL}}$$
$$= \frac{R_s(\sin\eta_L)(L_u - P_o)\sin\left(\arccos\left(\frac{(L_u - P_o)^2 + P_l^2 - (Y_{3L} - Y_{9L})^2 - (X_{9L} - X_{3L})^2}{2(L_u - P_o)P_l} \right) \right)}{R_p(\sin\gamma_L)\left(|X_{5L} - X_{3L}| + \frac{(X_1 - |X_{5L}|)(\cos\alpha_L(Y_{5L} - Y_{3L}) - \sin\alpha_L|X_{5L} - X_{3L}|)}{\cos(\alpha_L - SAI' + (\theta_L - \theta'))\sqrt{(X_{4L} - X_{5L})^2 + (Y_{5L} - Y_{4L})^2}} \right)}$$

(EQ 7-50)

7.34 Rocker-Arm Suspension Motion Ratio - Figures 7-7 describes the nomenclature which will be used to calculate the instantaneous motion ratio for rocker-arm type suspensions. A rocker-arm suspension is similar to a pull-rod suspension in that the tire forces are transferred to the spring through the upper kingpin ball joint. In the case of a rocker-arm suspension, the upper control arm transfers the tire force directly to the spring through a crank attached to the upper control arm at its inner pivot point. The upper control arm therefore replaces one half of the bell-crank, and the pull-rod is eliminated.

The analysis of the forces on the upper & lower kingpin pivot points is identical to the pull-rod method. Once the forces at the upper kingpin ball joint are known, they can be balanced against the spring moment by taking moments about the upper inner pickup point using (EQ 7-51) (CW=+):

$$F_{uy}|X_5 - X_3| + F_{ux}(Y_5 - Y_3) = F_s R_s(\sin\eta) \qquad \text{(EQ 7-51)}$$

The spring force can now be found by substituting (EQ 7-38) & (EQ 7-39) into (EQ 7-51) to produce (EQ 7-52):

$$F_s = \frac{(F_t - F_l\sin\alpha)|X_5 - X_3| + F_l\cos\alpha(Y_5 - Y_3)}{R_s(\sin\eta)}$$
$$= \frac{(F_t)|X_5 - X_3| + F_l(\cos\alpha(Y_5 - Y_3) - \sin\alpha|X_5 - X_3|)}{R_s(\sin\eta)} \qquad \text{(EQ 7-52)}$$

The spring/crank incident angle "η" is found through the law of cosines to be (EQ 7-53):

$$\eta = \arccos\left(\frac{S_l^2 + R_s^2 - (X_3 - X_{14})^2 - (Y_3 - Y_{14})^2}{2S_l R_s} \right) \qquad \text{(EQ 7-53)}$$

The angular position of the spring crank relative to the imaginary line connecting the inner pivot point of the upper control arm with the lower spring mount "ν" is given by (EQ 7-54):

$$\nu = \nu' - (\beta - \beta')$$
$$= \arccos\left(\frac{R_s^2 + (X'_3 - X'_{14})^2 + (Y'_3 - Y'_{14})^2 - (S'_l)^2}{2R_s\sqrt{(X'_3 - X'_{14})^2 + (Y'_3 - Y'_{14})^2}} \right) - (\beta - \beta')$$

(EQ 7-54)

where "ν'" is the static relative angular position of the spring crank, and $(\beta - \beta')$ is the upper control arm rotation (as measured from the static control arm angle "β'").

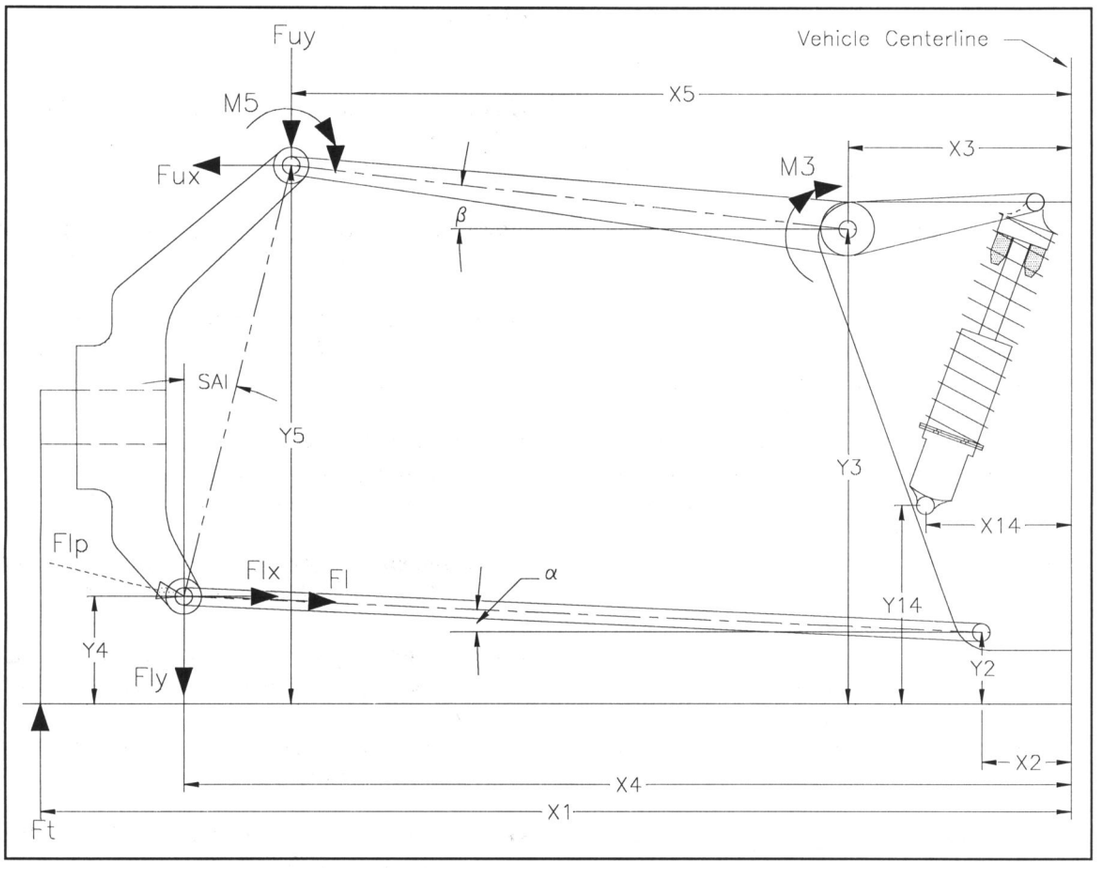

FIGURE 7-7

ROCKER ARM MOTION RATIO CALCULATION PARAMETERS

The spring length "S_l"can now be found through the law of cosines to be (EQ 7-55):

$$S_l=\sqrt{R_s^{\,2}+(X_3-X_{14})^2+(Y_3-Y_{14})^2-2R_s\cos v\sqrt{(X_3-X_{14})^2+(Y_3-Y_{14})^2}}$$

(EQ 7-55)

The spring force can now be found as a function of the tire force by substituting (EQ 7-35) into (EQ 7-52) to produce (EQ 7-56):

$$F_s=\frac{(F_t)\left(|X_5-X_3|+\dfrac{(X_1-|X_5|)(\cos\alpha(Y_5-Y_3)-\sin\alpha|X_5-X_3|)}{\cos(\alpha-SAI'+(\theta-\theta'))\sqrt{(X_4-X_5)^2+(Y_5-Y_4)^2}}\right)}{R_s(\sin\eta)}$$

(EQ 7-56)

In a rocker-arm suspension, "$ArmP$" becomes "L_u" and $(\sin\gamma)=1$. These variables therefore cancel out of the force ratio in (EQ 7-50). Equation 7-56 then leads directly to the instantaneous motion ratio for a rocker arm suspension defined by (EQ 7-57) (left shown, right is similar):

$$MR_{L(rocker-arm)}=\frac{F_{tL}}{F_{sL}}$$

$$=\frac{R_s(\sin\eta_L)}{|X_{5L}-X_{3L}|+\dfrac{(X_1-|X_{5L}|)(\cos\alpha_L(Y_{5L}-Y_{3L})-\sin\alpha_L|X_{5L}-X_{3L}|)}{\cos(\alpha_L-SAI'+(\theta_L-\theta'))\sqrt{(X_{4L}-X_{5L})^2+(Y_{5L}-Y_{4L})^2}}}$$

(EQ 7-57)

VIII MODELING USING COMPUTERS

These equations were used to write a steady-state vehicle simulation computer program which models the kinematic and dynamic behavior of vehicles which use the unequal length A arm suspensions typically found in purpose built road racing vehicles. This program calculates a vehicle's steady-state reactions to lateral, longitudinal & vertical accelerations, given basic design parameters.

This program was used to model the steady-state handling characteristics of a CART Indy car, IMSA GTS car and two Formula Fords. These four designs and their graphical simulation results are presented in Modeling Steady-state Suspension Kinematics & Vehicle Dynamics of Road Racing Cars, Part II: Examples (SAE Paper #942506).

IX SUMMARY

While these equations accurately model steady-state handling behavior, it should be noted that they ignore tire and bushing compliance, and linearize the equation for roll resistance/degree. While this linearization is reasonable for road racing vehicles, it can easily be removed when modeling vehicles which exhibit larger roll angles.

Due to the large number of interdependent equations required to accurately model steady-state handling behavior, obtaining a solution requires iterative calculation techniques. For example, when calculating the response of a vehicle with an outboard suspension to a +/- 1G bump/droop simulation, a solution that is accurate to 1/1000 of the stated units can be reached in less than 25 iterations. However, on vehicles with push or pull-rod suspensions the solution can require over 1000 iterations. This is due to the ability of bell-crank suspensions to produce large changes in wheel rate.

These large changes in motion ratio are a result of the sensitivity that push & pull-rod suspensions have on bell-crank rotation. As the iteration subroutine converges on a solution, small oscillations of the bell-crank can cause the motion ratio to change more quickly than the iteration engine can handle.

Therefore, when choosing a programming language to model steady state handling behavior using these equations, make sure that the available iteration subroutines allow adjustment of at least the convergence bandwidth and the iteration method. The requirement for such complex iterations can be reduced by assuming constant motion ratios. However, while this assumption is often made and results in quicker solutions, it is rarely reasonable in road racing cars (as described in section 7.30) and not recommended.

REFERENCES

Bastow, Donald. Car Suspension and Handling. London, England: Pentech Press Limited. 1990.

Campbell, Colin. New Directions in Suspension Design. Cambridge, MA: Robert Bently, Inc. 1986.

Cole, D. Elementary Vehicle Dynamics: course notes in Mechanical Engineering. Ann Arbor, MI: University of Michigan. 1972

Costin, Michael, and David Phipps. Racing and Sports Car Chassis Design. Cambridge, MA: Robert Bently, Inc. 1965.

Crahan, Thomas. Modeling Steady-state Suspension Kinematics & Vehicle Dynamics of Road Racing Cars: Part II: Examples (SAE paper #942506). Warrendale, PA: Society of Automotive Engineers, Inc. 1994.

Dixon, John C. Tyres, Suspension and Handling. Cambridge, England: Cambridge University Press. 1991.

Gillespie, Thomas D. Fundamentals of Vehicle Dynamics. Warrendale, PA: Society of Automotive Engineers, Inc. 1992.

Howard, Geoffrey. Chassis & Suspension Engineering. London, England: Osprey Publishing Limited. 1987.

Iacovoni, D. H. Fundamentals of Automobile Handling Analysis. Warrendale, PA: Society of Automotive Engineers, Inc. 1969.

Incandela, Sal. The Anatomy and Development of the Formula One Racing Car from 1975. Newbury Park, CA: Haynes Publications, Inc. 1986.

Mola, Simone. Fundamentals of Vehicle Dynamics. Detroit, MI: General Motors Institute. 1978.

Olley, Maurice. Suspension and Handling (Olley's Bible). Detroit, MI: Chevrolet Engineering Center. 1937.

Olley, Maurice. Notes on Suspensions. Detroit, MI: Chevrolet Engineering Center. 1961.

Olley, Maurice. Suspensions Notes II. Detroit, MI: Chevrolet Engineering Center. 1966.

Puhn, Fred. How To Make Your Car Handle. Tucson, AZ: H.P. Books. 1981.

Purdy, Alec. Discussions with. Los Angeles, CA: Ferret Inc. 1993,1994

SAE Vehicle Dynamics Committee. Vehicle Dynamics Terminology, SAE J670e. Warrendale, PA: Society of Automotive Engineers, Inc. 1978

Smith, Carroll. Prepare To Win. Fallbrook, CA: Aero Publishers, Inc, 1975.

Smith, Carroll. Tune To Win. Fallbrook, CA: Aero Publishers, Inc, 1978.

Staniforth, Allan. Competition Car Suspension: Design, Construction, Tuning. Somerset, England: Haynes Publishing Group. 1988

Terry, Len, and Alan Baker. Racing Car Design and Development. Cambridge, MA: Robert Bently, Inc. 1973.

Van Valkenburgh, Paul. Race Car Engineering & Mechanics 2nd. Ed. Seal Beach, CA: Van Valkenburgh, Co. 1986.

NOMENCLATURE

SIMULATION PARAMETERS

G_x	Lateral acceleration in "G's"
G_y	Vertical acceleration in "G's"
G_z	Longitudinal accelerations in "G's"
$1g$	Vertical acceleration due to gravity in "G's"

KINEMATIC VARIABLES

X	Horizontal distance from any point to the static vehicle centerline
X'	Static horizontal distance from any point to the static vehicle centerline
Y	Height of any point above the ground
Y'	Static height above the: A) chassis bottom (for points directly attached to the chassis) B) ground (for points not directly attached to the chassis)
X_L & X_R	Left and right values of each dimension respectively. Left values are negative, right are positive.
X_1	Average of the left & right absolute 1/2 track widths
X_{1L} & X_{1R}	Absolute value of 1/2 the left and right track widths
X_{1m}	1/2 of the mean track width
Y_1	Height of the chassis bottom above ground
X_2	Horizontal distance from the static vehicle centerline to the lower control arm inner pick up point
Y_2	Height of the lower control arm inner pickup point above ground
X_3	Horizontal distance from the static vehicle centerline to the upper control arm pick inner up point
Y_3	Height of the upper control arm inner pickup point above ground
X_4	Horizontal distance from the static vehicle centerline to the lower hub carrier (kingpin) ball joint
Y_4	Height of the lower hub carrier (kingpin) ball joint above ground
X_5	Horizontal distance from the static vehicle centerline to the upper hub carrier (kingpin) ball joint
Y_5	Height of the upper hub carrier (kingpin) ball joint above ground
X_6	Horizontal offset of the upper and lower hub carrier (kingpin) ball joints
Y_6	Height of the wheel spindle above ground
X_7	Horizontal distance from the static vehicle centerline to the instantaneous center
Y_7	Height of the instantaneous center above ground
X_8	Lateral displacement of the roll center away from the vehicle centerline
Y_8	Height of the roll center above ground
Y_{8m}	Height of the mean roll center above ground
X_9	Horizontal distance from the static vehicle centerline to the: A) upper outboard spring/damper pickup point (outboard spring suspension) B) push or pull-rod end which is connected to the bell-crank (push or pull-rod suspension)
Y_9	Height above ground of the: A) upper outboard spring/damper pickup point (outboard spring suspension) B) push or pull-rod end which is connected to the bell-crank (push or pull-rod suspension)
X_{10}	Horizontal distance from the static vehicle centerline to the outboard spring/damper or push-rod attachment point to the lower control arm

Y_{10}	Height above ground of the outboard spring/damper or push-rod attachment point to the lower control arm
X_{11}	Horizontal distance from the static vehicle centerline to the pull-rod attachment point to the upper control arm
Y_{11}	Height above ground of the pull-rod attachment point to the upper control arm
X_{12}	Horizontal distance from the static vehicle centerline to the push or pull-rod bell-crank pivot point
Y_{12}	Height of the push or pull-rod bell-crank pivot point above ground
X_{14}	Horizontal distance from the static vehicle centerline to the inboard spring mounting point
Y_{14}	Height of the inboard spring mounting point above ground
L_l	Lower control arm length
L_u	Upper control arm length
P_l	Push or pull-rod length
R_p	Bell-crank arm length on the push or pull-rod side
R_s	Bell-crank arm length on the spring side
H_{hc}	Hub carrier height
S_o	The offset of the lower spring/damper pickup point from the outer end of the lower control arm. This point is assumed to lie in-line with the control arm axis.
P_o	The offset of the push-rod (or pull-rod) pick up from the outer end of the lower (or upper) control arm. This point is assumed to lie in-line with the control arm axis.
ArmS	The moment arm through which the outboard spring produces its resisting torque about the lower control arm inner pickup point
ArmP	The moment arm through which the push-rod (or pull-rod) produces its resisting torque about the lower (or upper) control arm inner pickup point
D_m	Maximum chassis droop
α	The angle which the lower control arm makes with horizontal
β	The angle which the upper control arm makes with horizontal
χ	The angle which the imaginary line connecting the lower kingpin ball joint to the center of the tire contact patch makes with the ground
ε	The angle which the imaginary line connecting the upper kingpin ball joint to the center of the tire contact patch makes with the ground
ϕ	Vehicle roll angle
γ	The incident angle between the push or pull-rod and their bell-crank arm
η	The incident angle between the inboard spring axis and its bell-crank arm
ι	The incident angle between the push or pull-rod crank arm and the imaginary line connecting the bell-crank pivot point with the push or pull-rod attachment point to the control arm
θ	Wheel camber relative to ground
κ	The angle which the imaginary line connecting the bell-crank pivot point with the push or pull-rod attachment to the control arm makes with horizontal
λ	The angle which the push or pull-rod crank arm makes with horizontal
μ	Coefficient of friction
ν	The incident angle between the spring crank and the imaginary line connecting the: A) crank pivot point with the spring mounting point (push or pull-rod suspensions) B) upper control arm inner pivot point with the spring mounting point (rocker-arm suspensions)
ρ	The angle between the ground and the tire reaction force vector which acts on the roll center to cause jacking
SAI'	Static Steering Axis Inclination angle

DYNAMICS VARIABLES

M_s	Total sprung mass
M_{uf}	Front unsprung mass
M_{ur}	Rear unsprung mass
Y_{cg}	Height of the sprung mass c.g. above ground
Y_{uf}	Height of the front unsprung mass c.g. above ground
Y_{ur}	Height of the rear unsprung mass c.g. above ground
A	Longitudinal distance from the vehicle's c.g. to the front wheel centers
B	Longitudinal distance from the vehicle's c.g. to the rear wheel centers
F_t	Vertical tire force at the center of pressure
F_{tf} & F_{tr}	The additional front and rear vertical tire forces due to longitudinal load transfer
F_l	The force at the lower kingpin ball joint which acts parallel to the lower control arm
F_{lp}	The force at the lower kingpin ball joint, which acts perpendicular to the imaginary line that connects the upper & lower kingpin ball joints
F_{lx} & F_{ly}	The horizontal and vertical force components which act at the lower kingpin ball joint
F_u	The force at the upper kingpin ball joint which acts parallel to the upper control arm
F_{up}	The force at the upper kingpin ball joint, which acts perpendicular to the imaginary line that connects the upper & lower kingpin ball joints
F_{ux} & F_{uy}	The horizontal and vertical force components which act at the upper kingpin ball joint
F_s	Spring force
F_p	Push or pull-rod force
F_{jL} & F_{jR}	Left and right vertical components of the tire reaction force vectors which act on the roll center to cause jacking
F_j	Jacking force
LT_x	Lateral load transfer
LT_z	Longitudinal load transfer
RR_f	Front roll resistance
RR_r	Rear roll resistance
RR_t	Total roll resistance
RR/deg	Roll resistance per degree
$MR_{(outboard-spring)}$	*Instantaneous* spring motion ratio for an outboard spring suspension
$MR_{(push-rod)}$	*Instantaneous* spring motion ratio for a push-rod suspension
$MR_{(pull-rod)}$	*Instantaneous* spring motion ratio for a pull-rod suspension
$MR_{(rocker-arm)}$	*instantaneous* spring motion ratio for a rocker arm suspension
MR_{rb}	*Instantaneous* anti-roll bar motion ratio
δ_w	Wheel deflection
K_w	*Instantaneous* wheel rate

SPRING DESIGN PARAMETERS

K_s	Spring rate
N	Number of active spring coils
d	Diameter of the spring wire
D	Spring coil diameter as measured from wire center to wire center
G	Modulus of rigidity of the spring material
S_l' & S_l	Static and *instantaneous* spring length
δ_s	Spring deflection

ANTI-ROLL BAR DESIGN PARAMETERS

K_{rb}	Spring constant for the anti-roll bar assembly (blades & torque tube)
K_{bl}	Spring constant of the tapered blade in its stiffest vertical position
l	Anti-roll bar blade length
b	Anti-roll bar blade thickness
H_r	Anti-roll bar blade height at the root (connection to the torque tube)
H_t	Anti-roll bar blade height at the tip
A	Cross sectional area of the anti-roll bar blade at a point "x" from the blade tip along its length (equal to "bH")
δ_{bl}	Anti-roll bar blade tip deflection due to bending
V	Shear force in the anti-roll bar blade
G	Modulus of rigidity of the anti-roll bar blade material
M	Bending moment of the anti-roll bar blade
E	Modulus of elasticity of the anti-roll bar blade material
I	Moment of inertia at a point "x" from the blade tip along its length
k	Correction coefficient for strain energy due to shear
K_{tt}	Linear spring constant of the anti-roll bar torque tube
d_o	Anti-roll bar torque tube outer diameter
d_i	Anti-roll bar torque tube inner diameter
L	Length of the anti-roll bar torque tube from end to end (*true length*)
G	Torsional modulus of the anti-roll bar torque tube material

ACKNOWLEDGMENTS

This paper is dedicated to my wife Laura; without whose unwavering support and endless patience, this work would not have been possible.

I would also like to express my sincere thanks to Alec Purdy for sharing the wealth of his road racing development knowledge, and guiding me as I struggled to understand the subtleties of vehicle handling behavior and describe them in mathematical terms. I would like to thank Bruce Eklund, Dean Case, Marcus Crahan III, Ross Iwamoto, Matthew Bornyasz, and Alec Purdy for their diligence in reviewing this work. Copies of Maurice Olley's pioneering works on this subject were kindly provided by General Motors and Paul Van Valkenburgh.